Eur. Phys. J. C 56, 203–219 (2008)
DOI 10.1140/epjc/s10052-008-0655-x

THE EUROPEAN PHYSICAL JOURNAL C

Regular Article – Theoretical Physics

# Generalized parton distributions and deeply virtual Compton scattering in color glass condensate model

K. Goeke[1,a], V. Guzey[2,b], M. Siddikov[1,3,c]

[1] Institut für Theoretische Physik II, Ruhr-Universität-Bochum, Universitätsstraße 150, 44780 Bochum, Germany
[2] Theory Center, Jefferson Lab, Newport News, VA 23606, USA
[3] Theoretical Physics Department, Uzbekistan National University, Tashkent 700174, Uzbekistan

Received: 2 May 2008 /
Published online: 5 July 2008 – 

**Abstract.** Within the framework of the color glass condensate model, we evaluate quark and gluon generalized parton distributions (GPDs) and the cross section of deeply virtual Compton scattering (DVCS) in the small-$x_{\rm B}$ region. We demonstrate that the DVCS cross section becomes independent of energy in the limit of very small $x_{\rm B}$, which clearly indicates saturation of the DVCS cross section. Our predictions for the GPDs and the DVCS cross section at high energies can be tested at the future Electron–Ion Collider and in ultra-peripheral nucleus–nucleus collisions at the LHC.

**PACS.** 12.38.Mh; 13.60.Fz; 13.85.Fb; 24.85.+p; 25.20.Dc

## 1 Introduction

During the last decade hard exclusive reactions, such as deeply virtual Compton scattering (DVCS), $\gamma^*(q)+p\to\gamma(q')+p'$, have been a subject of intensive theoretical and experimental studies [1–16]. Particular interest has been attached to the generalized Bjorken kinematics,

$$\begin{aligned} -q^2 &= Q^2 \quad \text{large}\,,\\ W^2 &= (P+q)^2 \quad \text{large}\,,\\ x_{\rm B} &= \frac{Q^2}{2P\cdot q} = \text{const}\,,\\ t &= \Delta^2 = (P'-P)^2 \ll Q^2\,, \end{aligned} \tag{1}$$

where $q$ is the momentum of the virtual photon, $P$ is the initial momentum of the target hadron, $P'$ is the final momentum of the target, and $t$ is the momentum transfer.

In this kinematics the DVCS amplitude is factorized [7,8] into the convolution of the perturbative coefficient function with nonperturbative generalized parton distributions (GPDs) of the target. Recently, leading-twist dominance (validity of the collinear QCD factorization) in DVCS on the proton target was demonstrated by the Hall A Collaboration at Jefferson Laboratory [17], already at rather low values of $Q^2$, $1.5\,\text{GeV}^2 \le Q^2 \le 2.3\,\text{GeV}^2$.

However, it turns out that in experiments with nuclei the virtuality $Q^2$ is not always very large, and one cannot say how accurate the predictions based on factorization are, or, in other words, how large the higher-twist corrections are. One of the examples, where this approach cannot be applied, is DVCS on the nuclei measured by HERMES Collaboration in DESY [18]. Due to the small values of $Q^2 \sim 1$–$2\,\text{GeV}^2$ one has to use other effective models, e.g. a generalized vector meson dominance model (GVMD) [19].

At very large $W^2$ (very small values of $x_{\rm B}$), the perturbative collinear factorization is expected to break down due to the high densities of the partons [20]. Even for relatively large values of $Q^2$ when the running coupling constant of the strong interactions $\alpha_{\rm s}(Q^2)$ is small, the effective expansion parameter $\alpha_{\rm s}(Q^2)g(x,Q^2)$, where $g(x,Q^2)$ is the gluon density in the target, becomes large. This invalidates the perturbative expansion leading to the collinear factorization. Since in heavy nuclei the parton densities are enhanced by the atomic number $A$ compared to those in the nucleon, the onset of the effects associated with high parton densities may take place at the values of $x_{\rm B}$ which will already be achieved at the future Electron–Ion Collider (EIC).

In this paper we use the framework of the color glass condensate (CGC) model offered in [21,22] (see also recent reviews [23–27]). We generalize the formalism of the CGC model to exclusive reactions and evaluate the generalized parton distributions (GPDs) and the DVCS amplitude at small $x_{\rm B}$. We find that for DVCS off heavy nuclei, the DVCS cross section is virtually $x_{\rm B}$-independent, i.e. the DVCS cross section *saturates* in the small-$x_{\rm B}$ limit. The general saturation property built-in into this model is an essentially nonperturbative effect, which complies with the

[a] e-mail: Klaus.Goeke@tp2.rub.de
[b] e-mail: VGuzey@jlab.org
[c] e-mail: Marat.Siddikov@tp2.rub.de

general Froissart (unitarity) bound [28–31]

$$F_2(x,Q^2) \le \ln^n(s) \sim \ln^n\left(\frac{1}{x}\right), \tag{2}$$

where $n=3$ for DIS on nucleons; $n=1$ for DIS on heavy nuclear targets. This should be compared to the Froissart bound for the case of hadron–hadron scattering, $\sigma \le \ln^2 s$.

For comparison, estimates of the $x$-dependence based on the perturbative evolution equations do not possess saturation: DGLAP predicts a fast growing $x$-dependence [32, 33]:

$$xg(x,Q^2) \sim \exp\left(4\sqrt{\frac{3}{\pi}\alpha_{\rm s}(Q^2)\ln\frac{Q^2}{Q_0^2}\ln\frac{1}{x}}\right), \tag{3}$$

and the BFKL framework [23, 34–40] predicts the power $x$-dependence

$$xg(x,Q^2) \sim \left(\frac{1}{x}\right)^{4\alpha_{\rm s}(Q^2)\ln 2}. \tag{4}$$

The crucial parameter of the CGC model is the saturation scale $Q_{\rm s}^2(x,A)$, which gives the threshold for the transition to the saturation regime. The saturation scale $Q_{\rm s}^2(x,A)$ comes into play as a universal parameter in many tasks. For example, in a CGC explanation of geometric scaling [41] in DIS data from HERA, the structure function $F_2(x,Q^2)$ is represented as a function of only one variable, i.e. $F_2(x,Q^2) = f\left(\frac{Q^2}{Q_{\rm s}^2(x)}\right)$.

The paper is organized as follows. In Sect. 2.1 we give a brief overview of the model used for the evaluations. In particular, we generalize the original framework of [21, 22] to the finite nucleus case in order to consider the off-forward matrix elements. In Sect. 3 we evaluate the quark GPDs, and in Sect. 4 we evaluate the DVCS amplitude. In Sect. 5 we present our results and draw conclusions.

## 2 Generalized parton distributions in the color glass condensate model

### 2.1 Overview of the color glass condensate model

The basic assumption of CGC is that one can separate the partons into fast ($x_{\rm B} \sim 1$) and slow ($x_{\rm B} \ll 1$) ones, according to their light-cone fraction $p^+$. The former are considered as classical "sources", and the latter are the dynamical degrees of freedom in the model. In the leading order of $\alpha_{\rm s}(Q^2)$, one has just ordinary Yang–Mills equations for the gluon fields, in NLO one has a standard loop expansion. It is assumed that the dynamics of the "fast" partons does not depend on the "slow" partons; thus, the configurations of the fast partons are *random* and one must *average* over all possible configurations of these "sources" $J_\mu^a(x) = \delta_{\mu+}\rho^a(x)$, where $a$ is a color index, and $x$ is a coordinate. The weight functional $W[\rho]$ encodes the dynamics of the "fast" subsystem and comes as an external parameter in the model. There are no restrictions on this functional except for the obvious gauge and Lorentz invariance. The additional requirement of color neutrality,

$$\int {\rm d}^3x \langle \rho^a(\mathbf{x})\rho^b(\mathbf{0})\rangle = 0\,, \tag{5}$$

was introduced in [42]. It reflects the fact that the physical states are colorless.

If we define $x_0$ as the scale which separates "fast" and "slow" partons, then the dependence of the functional $W[\rho]$ on the scale $x_0$ will be described by a kind of "renormalization group equation":

$$\frac{\partial W[\rho;\tau]}{\partial\tau} = \frac{1}{2}\int {\rm d}\mathbf{x}\,{\rm d}\mathbf{y}\frac{\delta}{\delta\rho^a(\mathbf{x})}\chi(\mathbf{x},\mathbf{y})\frac{\delta}{\delta\rho^b(\mathbf{y})}W[\rho;\tau]\,, \tag{6}$$

where $\tau = \ln\left(\frac{1}{x_0}\right)$ and $\chi(\mathbf{x},\mathbf{y})$ is a complicated functional of the field $\rho$.

While in the general case this equation has not been solved so far, there are known solutions for some special (asymptotic) cases. Conventionally $W[\rho]$ is chosen in Gaussian form [21, 22, 24]:

$$W[\rho] = \mathcal{N}\exp\left(-\frac{1}{2}\int {\rm d}\mathbf{x}\,{\rm d}\mathbf{y}\frac{\rho^a(\mathbf{x})\rho^a(\mathbf{y})}{\lambda(\mathbf{x},\mathbf{y})}\right), \tag{7}$$

where $\mathcal{N}$ is the normalization factor fixed from the condition $\int \mathcal{D}\rho W[\rho] = 1$ and the function $\lambda(\mathbf{x},\mathbf{y})$ is either a constant or a function fixed with some additional assumptions. Physically the function $\lambda(\mathbf{x},\mathbf{y})$ describes the correlation of the partons inside the target. It is obvious that in infinite nuclear matter it may depend only on the relative distance, i.e.

$$\lambda(\mathbf{x},\mathbf{y}) = \mu_A^2(\mathbf{x}-\mathbf{y})\,. \tag{8}$$

In the general case, the shape of the function $\mu_A^2(\mathbf{r})$ is unknown. However, the color neutrality condition (5) and the requirement that in the low parton density limit the model should reproduce BFKL predictions (4) fix the short-distance and large-distance behaviour. It was proposed in [24] that one may use the interpolation

Parameterization I:

$$\begin{aligned}\mu_A^2(\mathbf{r}) &= \int \frac{{\rm d}^2k}{(2\pi)^2}\mu^2(k){\rm e}^{-{\rm i}\mathbf{kr}} \\ &= \int \frac{{\rm d}^2\mathbf{k}}{(2\pi)^2}{\rm e}^{-{\rm i}\mathbf{kr}}\frac{k_\perp^2}{\pi}\frac{\left(\frac{Q_{\rm s}^2(x)}{k_\perp^2}\right)^\gamma}{1+\left(\frac{Q_{\rm s}^2(x)}{k_\perp^2}\right)^\gamma}\,,\end{aligned} \tag{9}$$

where $\gamma = \frac{1}{2}\sqrt{1+\frac{8\ln 2}{7\zeta(3)}} \approx 0.644$ is a numerical coefficient.

There are also simpler versions of the model [21, 22], which neglect the correlation of the partons, i.e.

$$\text{Parameterization II:} \qquad \frac{1}{\lambda(\mathbf{x},\mathbf{y})} = \frac{\delta(\mathbf{x}-\mathbf{y})}{\lambda_A(x^-)}\,, \tag{10}$$

where $\lambda_A(x^-)$ is some function.[1] In subsequent sections we will consider a first evaluation with the simple parameterization (10), and after that we discuss how the results change for the parameterization (9).

The choice of the Gaussian parameterization (7) enables us to evaluate all the results analytically. Notice, however, that (7) is explicitly $C$-even, i.e. the number of quarks is equal to the number of antiquarks *inside any target* in this model. This agrees with the experimental fact that the quark and antiquark parton densities are approximately equal at small $x_{\mathrm{B}}$. On the other hand, the $C$-parity of (7) implies that the model does not distinguish matter and antimatter and is not applicable to the evaluation of some quantities. For example, the baryon number and electric charge of the target are exactly zero, since they are due to the valence quarks.

An interesting generalization of the Gaussian parameterization (7) was discussed in [44]. In particular, it was found that for the model of $k \gg 1$ independent noninteracting quarks the distribution is indeed Gaussian, and the first correction is proportional to $\sim d_{abc} \int \mathrm{d}^3x \rho^a(\mathbf{x})\rho^b(\mathbf{x})\rho^c(\mathbf{x})$, where $d_{abc}$ is defined by the anticommutator of the generators $T^a$ of the group, $\{T^a, T^b\} = 2d_{abc}T^c$. However, for the DVCS and singlet GPDs discussed in this paper the $C$-odd correction does not contribute.

It is well known that at high energies, the real part of scattering amplitudes is suppressed by the slow energy dependence of the amplitude compared to the imaginary part [45–48]. Therefore, it is sufficient to consider only the imaginary part. Actually, as we shall show in Sect. 4, the real part of the DVCS amplitude in the CGC model is exactly zero.

The generating functional of the model has the form[2]

$$Z[j] = \int D\rho W[\rho] \frac{\int DA\delta(A^+)\mathrm{e}^{\mathrm{i}S[A,\rho]-\int \mathrm{d}xj\cdot A}}{\int DA\delta(A^+)\mathrm{e}^{\mathrm{i}S[A,\rho]}}, \quad (11)$$

where $S[A,\rho] = S[A] + \int \mathrm{d}\mathbf{x}\rho^a(\mathbf{x})A^a_-(\mathbf{x})$ and we used the light-cone gauge $n\cdot A = 0$, $n^2 = 0$. In order to restore the explicit gauge invariance of the action $S[A,\rho]$, the interaction term $\int \mathrm{d}\mathbf{x}\rho^a(\mathbf{x})A_-(\mathbf{x})$ is sometimes replaced with $\mathrm{Tr}\int \mathrm{d}^3\mathbf{x}\rho(\mathbf{x})W[A,\mathbf{x}]$, where

$$W[A,\mathbf{x}] = P\exp\left(\mathrm{i}g\int_{-\infty}^{x^+}\mathrm{d}\zeta A^+(\zeta)\right) \quad (12)$$

is the Wilson link.

[1] From the physical point of view, the nucleus moving with ultrarelativistic velocity in the laboratory frame is strongly squeezed due to Lorentz contraction, the observer sees only a thin "pancake" with (almost) uniform width and (almost infinite) radius $R$. This explains the choice of the parameterization (10), where $\lambda_A(x^-)$ in the previous formula must be strongly peaked around $x^- \approx 0$. Quite often, for simplicity it is assumed that the width might be completely neglected. A very interesting generalization of the framework to the finite width case may be found in [43].

[2] For the sake of brevity we included only gluons. Addition of the quark sector is trivial.

### 2.2 Finite nucleus

Since in this paper we are interested in DVCS, an off-forward reaction, we can no longer use the infinite nuclear matter approximation. Indeed, the DVCS cross section off a nuclear target rapidly decreases as one increases the momentum transfer $t$. As a result, sizable cross sections exist only for $|t| \sim 1/R_A^2$, where $R_A$ is the nuclear radius. In the infinite nuclear matter, all the off-forward cross sections vanish.[3] This means that we have to take into account the off-forward kinematics from the very beginning. If the coordinate of the nucleus center of mass is $\mathbf{X}$, then the weight functional $W[\rho]$ may be chosen as

$$W_\rho[\rho,\mathbf{X}] = \exp\left\{-\frac{1}{2}\int \mathrm{d}^3x\theta(|\mathbf{x}_\perp - \mathbf{X}_\perp| < R_A) \times \frac{\rho^a(\mathbf{x}-\mathbf{X})\rho^a(\mathbf{x}-\mathbf{X})}{\lambda_A(x^- - X^-)}\right\}, \quad (13)$$

where we extracted the "zero mode" (integration over the nucleus center of mass) explicitly according to standard technique [49] and introduced an explicit cutoff factor $\theta(|\mathbf{x}_\perp - \mathbf{X}_\perp| < R_A)$ which forbids the *color condensate* $\rho^a(\mathbf{x})$ from outside of the nucleus. The cutoff in $x^-$ is provided by the factor $\lambda_A(x^- - X^-)$. The interaction of gluons with the condensate is also modified by this cutoff factor:

$$S[A,\rho] = S[A] + \mathrm{Tr}\int \mathrm{d}^3x\theta(|\mathbf{x}_\perp - \mathbf{X}_\perp| < R_A)\rho(\mathbf{x})A_-(\mathbf{x}) \quad (14)$$

for the linear interaction, or

$$S[A,\rho] = S[A] + \mathrm{Tr}\int \mathrm{d}^3x\theta(|\mathbf{x}_\perp| < R_A)\rho(\mathbf{x})W[A](\mathbf{x}) \quad (15)$$

for the interaction via Wilson link (12). The generating functional (11) takes the form

$$Z[j] = \int D\rho \mathrm{d}X \mathrm{e}^{\mathrm{i}\boldsymbol{\Delta}\mathbf{X}} W[\rho,\mathbf{X}] \frac{\int DA\delta(A^+)\mathrm{e}^{\mathrm{i}S[A,\rho]-\int \mathrm{d}xj\cdot A}}{\int DA\delta(A^+)\mathrm{e}^{\mathrm{i}S[A,\rho]}}. \quad (16)$$

Notice that the formal introduction of the $\theta$-functions is equivalent to the redefinition of the functional integral:

$$\int D\rho := \prod_x \mathrm{d}\rho(x^-, |\mathbf{x}_\perp - \mathbf{X}_\perp| < R_A)\,\mathrm{d}^3X\,. \quad (17)$$

Indeed, configurations with $\rho(|\mathbf{x}_\perp| > R_A) \neq 0$ do not interact with anything and thus contribute only to the normalization constant.

Since the coupling constant $\alpha_{\mathrm{s}}$ is small, we can take the integral over the gluon field $A_\mu$ in (11) in the saddle-point

[3] Technically, we get the prefactors $\delta(\boldsymbol{\Delta})$ for all observables in the original framework of [21, 22] in the infinite nuclear matter limit.

approximation. In the leading order, the gluon field $A_\mu$ is just the solution of the equation of motion

$$D_\mu F_a^{\nu\mu}(x) = \delta^{\nu,+}\delta(x^-)\rho^a(x_\perp)\,, \tag{18}$$

where $\rho^a(x_\perp)$ is an arbitrary external field, and the additional gauge constraint $A^+ = 0$ is implied. Notice that we do not impose any conditions onto the gluonic fields $A_\mu^a$ at the large distance $|\mathbf{x}| > R_A$. The solution of (18) is [24]

$$A^\mu = U\left(\tilde{A}_\mu + \frac{\mathrm{i}}{g}\partial_\mu\right)U^\dagger\,, \tag{19}$$

where[4]

$$\tilde{A}_\mu = \delta^{\mu+}\alpha(x^-, x_\perp)\,, \tag{20}$$

$$U = P\exp\left\{\mathrm{i}g\int_{-\infty}^{x^-}\mathrm{d}z^-\alpha_a(z^-, x_\perp)T^a\right\}, \tag{21}$$

$$\begin{aligned}\alpha(x^-, x_\perp) &= \frac{1}{-\partial_\perp^2}\tilde{\rho}\\ &= \int \mathrm{d}^2y_\perp \frac{1}{4\pi}\ln\frac{1}{(x_\perp - y_\perp)^2\Lambda_{\mathrm{QCD}}^2}\tilde{\rho}(x^-, y_\perp)\,,\end{aligned} \tag{22}$$

$$\tilde{\rho}(x^-, x_\perp) = U^\dagger(x^-, x_\perp)\rho(x^-, x_\perp)U(x^-, x_\perp)\,, \tag{23}$$

and $T^a$ are the generators of the color group.

The analytical solution (19) enables us to evaluate different correlators. A straightforward evaluation of the $\langle\rho\rho\rangle$-correlator with the weight function (13) yields

$$\begin{aligned}\langle P'|\rho(\mathbf{x})\rho(\mathbf{y})|P\rangle &= \bar{P}^+\int \mathrm{d}^3X\mathrm{e}^{\mathrm{i}\boldsymbol{\Delta}\mathbf{X}}\theta(|\mathbf{x}_\perp - \mathbf{X}_\perp| < R_A)\\ &\quad\times\lambda_A(x^- - X^-)\delta^3(\mathbf{x}-\mathbf{y})\\ &= f(\Delta)\bar{P}^+\mathrm{e}^{-\mathrm{i}\boldsymbol{\Delta}\mathbf{x}}\delta^3(\mathbf{x}-\mathbf{y})\,,\end{aligned} \tag{24}$$

where

$$f(\Delta) = \left(\tilde{\lambda}(\Delta^+) \equiv \int \mathrm{d}x^-\lambda(x^-)\mathrm{e}^{-\mathrm{i}x^-\Delta^+}\right)f_\perp(\Delta_\perp)\pi R_A^2\,, \tag{25}$$

and

$$\begin{aligned}f_\perp(\Delta_\perp) &= \frac{1}{\pi R_A^2}\int \mathrm{d}^2x_\perp\theta(|\mathbf{x}_\perp| < R_A)\mathrm{e}^{\mathrm{i}\boldsymbol{\Delta}_\perp\mathbf{x}_\perp}\\ &= \frac{J_1(\Delta_\perp R_A)}{\Delta_\perp R_A}\,.\end{aligned} \tag{26}$$

We can see that for any fixed non-zero $\Delta_\perp \neq 0$ the result vanishes in the $R_A \to \infty$ limit in agreement with the discussion at the beginning of this section. The evaluation of the gluonic GPDs defined by [11]

$$\begin{aligned}&xH^g(x,\xi,t) =\\ &\quad\frac{1}{\bar{P}^+}\int \mathrm{d}z^-\mathrm{e}^{\mathrm{i}x\bar{P}^+}\left\langle P'\middle|F_{+k}^a\left(-\frac{z^-}{2}\right)F_+^{k,a}\left(-\frac{z^-}{2}\right)\middle|P\right\rangle\end{aligned} \tag{27}$$

is done in a quasiclassical approximation,

$$\begin{aligned}xH^g(x,\xi,t) \approx \int \mathrm{d}^3X\mathrm{e}^{\mathrm{i}\boldsymbol{\Delta}\mathbf{X}}\int \mathrm{d}z^-\mathrm{e}^{\mathrm{i}x\bar{P}^+z^-}\\ \times F_{+k}^a\left(-\frac{z^-}{2} - \mathbf{X}\right)F_+^{k,a}\left(\frac{z^-}{2} - \mathbf{X}\right),\end{aligned} \tag{28}$$

where $F_{\mu\nu}$ in the r.h.s. of (28) corresponds to the classical solution found in the previous subsection. Evaluation of (28) [24] gives[5]

$$\begin{aligned}xH^g(x,\xi,t) &= \frac{\left(N_c^2-1\right)}{\bar{P}^+}\int \mathrm{d}^3X\mathrm{e}^{\mathrm{i}\boldsymbol{\Delta}\mathbf{X}}\\ &\quad\times\left(\int \mathrm{d}^3\tilde{\Delta}\mathrm{e}^{-\mathrm{i}\tilde{\Delta}\mathbf{X}}\left(-\partial_{r_\perp}^2\right)\tilde{\gamma}_A(x^-, \mathbf{r}_\perp; \tilde{\Delta})\right)\\ &\quad\times\exp\left[-g^2N_c\left(\frac{\tilde{f}\left(\mathbf{0}, \frac{\mathbf{r}}{2} - \mathbf{X}\right) + \tilde{f}\left(\mathbf{0}, -\frac{\mathbf{r}}{2} - \mathbf{X}\right)}{2}\right.\right.\\ &\quad\left.\left. - \tilde{f}(\mathbf{r}, -\mathbf{X})\right)\right]_{r_\perp \approx 1/Q},\end{aligned} \tag{29}$$

where

$$\tilde{f}(\mathbf{r}_1, \mathbf{r}_2) = \int \frac{\mathrm{d}^2\tilde{\Delta}}{(2\pi)^2}\mathrm{e}^{-\mathrm{i}\tilde{\Delta}\mathbf{r_2}}\int_{-\infty}^{+\infty}\mathrm{d}z^-\tilde{\gamma}_A(z^-, \mathbf{r}_1; \tilde{\Delta})\,, \tag{30}$$

and $\tilde{\gamma}_A(x^-, \mathbf{r}_\perp)$ is defined as

$$\begin{aligned}&f(\Delta)\bar{P}^+\int \frac{\mathrm{d}^3k}{(2\pi)^3}\frac{\mathrm{e}^{-\mathrm{i}\mathbf{x}(\mathbf{k}+\boldsymbol{\Delta}/2)}\mathrm{e}^{\mathrm{i}\mathbf{y}(\mathbf{k}-\boldsymbol{\Delta}/2)}}{\left(\mathbf{k}_\perp - \frac{\boldsymbol{\Delta}_\perp}{2}\right)^2\left(\mathbf{k}_\perp + \frac{\boldsymbol{\Delta}_\perp}{2}\right)^2} =\\ &\quad\delta(x^- - y^-)\tilde{\gamma}_A(x^-, \mathbf{x}_\perp - \mathbf{y}_\perp)\mathrm{e}^{\mathrm{i}\boldsymbol{\Delta}(\mathbf{x}+\mathbf{y})/2}\,.\end{aligned} \tag{31}$$

As one can see from (29), the gluon GPD $H^g(x,\xi,t)$ has a trivial $x$-dependence, $1/x$, for all $(\xi, t)$, since $x$ does not enter the right-hand side of (29). Physically, the exponent in (29) takes into account effects nonlinear in $\alpha_\mathrm{s}$ in the model.

### 2.3 Alternative kernel

In this section we discuss how all the previous formulae change with an alternative weight function (9). The weight

[4] The most interesting properties of the solution are the following. (1) Only transverse components of $A_\mu$ are not zero: $A_k = \frac{\mathrm{i}}{g}U\partial_k U^\dagger$, $k = 1, 2$. (2) $A_i \to 0$ for $x^- \to -\infty$. (3) The only non-zero components of $F^{\mu\nu}$ are $F^{+k} = -U\partial_k\alpha_a T^a U^\dagger$. (4) In the linear approximation, one should just drop the unitary matrices $U, U^\dagger$ to get $F^{+k} \approx -\partial_k\alpha_a T^a$.

[5] We omitted here a tedious, although quite simple evaluation. The interested reader may find the logic of the evaluation in [24], generalization to the off-forward case is done in Appendix B.

functional in this case should be written

$$W_\rho[\rho,X]=\mathcal{N}\exp\left\{-\frac{1}{2}\int \mathrm{d}^3x\theta(|\mathbf{x}_\perp-\mathbf{X}_\perp|<R_A)\times\frac{\rho^a(\mathbf{x}-\mathbf{X})\rho^a(\mathbf{y}-\mathbf{X})}{\mu_A^2(\mathbf{x}-\mathbf{y})}\right\}, \tag{32}$$

where the function $\mu_A^2(\mathbf{z})$ describes the correlation of the hadrons inside the nuclei and was defined in (9). Performing the evaluation as was discussed in Sect. 2.2, we obtain

$$\begin{aligned}\langle P'|\rho(\mathbf{x})\rho(\mathbf{y})|P\rangle &= \int \mathrm{d}X\mathrm{e}^{\mathrm{i}\boldsymbol{\Delta}\mathbf{X}}\theta(|\mathbf{x}_\perp-\mathbf{X}_\perp|\le R_A)\\ &\quad\times\theta(|\mathbf{y}_\perp-\mathbf{X}_\perp|\le R_A)\mu_A^2(\mathbf{x}_\perp-\mathbf{y}_\perp)\\ &= f(\mathbf{x}-\mathbf{y},\Delta)\mathrm{e}^{\mathrm{i}\boldsymbol{\Delta}\frac{\mathbf{x}+\mathbf{y}}{2}}\mu_A^2(\mathbf{x}-\mathbf{y})\\ &= \int\frac{\mathrm{d}^3k}{(2\pi)^3}\tilde{\mu}_A^2(\mathbf{k})\mathrm{e}^{-\mathrm{i}\mathbf{x}(\mathbf{k}+\boldsymbol{\Delta}/2)}\mathrm{e}^{\mathrm{i}\mathbf{y}(\mathbf{k}-\boldsymbol{\Delta}/2)},\end{aligned} \tag{33}$$

where

$$\tilde{\mu}_A^2(\mathbf{k})=\int \mathrm{d}^2\rho\mathrm{e}^{-\mathrm{i}\mathbf{k}\rho}f(\rho,\Delta)\mu_A^2(\rho), \tag{34}$$

$$\begin{aligned}f(\rho,\Delta) &= \int \mathrm{d}^2X\mathrm{e}^{\mathrm{i}\boldsymbol{\Delta}\mathbf{X}}\theta\left(\left|\frac{\rho}{2}-\mathbf{X}_\perp\right|\le R_A\right)\\ &\quad\times\theta\left(\left|\frac{\rho}{2}+\mathbf{X}_\perp\right|\le R_A\right)\\ &= \int\frac{\mathrm{d}^2k}{(2\pi)^2}\mathrm{e}^{-\mathrm{i}\mathbf{k}\rho}\phi\left(\mathbf{k}+\frac{\boldsymbol{\Delta}}{2}\right)\phi\left(\mathbf{k}-\frac{\boldsymbol{\Delta}}{2}\right),\end{aligned} \tag{35}$$

$$\phi(\mathbf{k})=\pi R_A^2\frac{2J_1(kR_A)}{kR_A}. \tag{36}$$

From (33) we can see that in finite nuclei the color neutrality condition (5) implies that we have to identify $\mu_A^2$ from (9) with $\tilde{\mu}_A^2(r)$. For $\tilde{\gamma}_A(x^-,\mathbf{r}_\perp)$ we can immediately obtain

$$\begin{aligned}\langle P'|\alpha(\mathbf{x})\alpha(\mathbf{y})|P\rangle &= \ldots\\ &= \int\frac{\mathrm{d}^3k}{(2\pi)^3}\tilde{\mu}_A^2(\mathbf{k})\frac{\mathrm{e}^{-\mathrm{i}\mathbf{x}(\mathbf{k}+\boldsymbol{\Delta}/2)}\mathrm{e}^{\mathrm{i}\mathbf{y}(\mathbf{k}-\boldsymbol{\Delta}/2)}}{\left(\mathbf{k}_\perp-\frac{\boldsymbol{\Delta}_\perp}{2}\right)^2\left(\mathbf{k}_\perp+\frac{\boldsymbol{\Delta}_\perp}{2}\right)^2}\\ &= \delta(x^--y^-)\tilde{\gamma}_A(x^-,\mathbf{x}_\perp-\mathbf{y}_\perp)\mathrm{e}^{\mathrm{i}\boldsymbol{\Delta}(\mathbf{x}+\mathbf{y})/2}.\end{aligned} \tag{37}$$

Thus we can see that this kernel differs from the previous one only by an additional factor $\tilde{\mu}^2(\mathbf{k})$ in the integrand.

### 2.4 Quark propagator in the CGC field

Although for the evaluation of the DVCS amplitude one may use the color dipole approximation, in this paper we evaluate the GPDs and the Compton amplitudes directly. In diagrammatic language this corresponds to a summation of all[6] the multigluon diagrams, whereas the color dipole approach assumes either only a Born term contribution or an eikonal approximation, as is shown by Fig. 1.

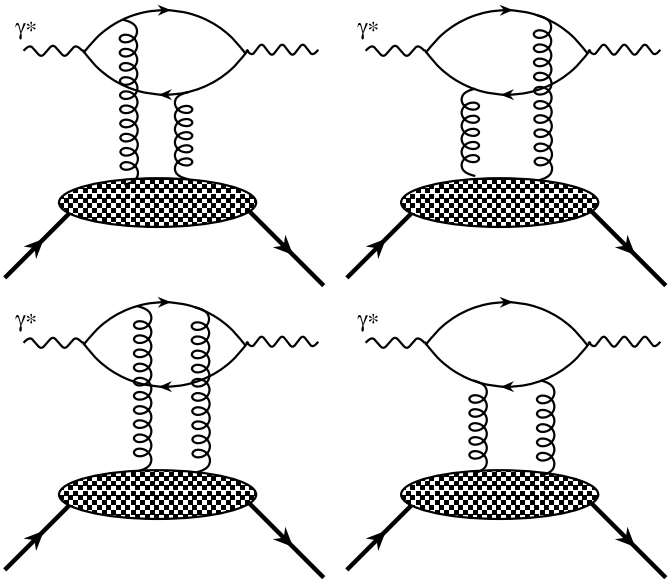


**Fig. 1.** Diagrams contributing to DVCS in the color dipole approximation. See [50] for an example of a DIS evaluation in this approach

For the evaluation of the quark GPDs in the leading order in $\alpha_\mathrm{s}(Q^2)$, we need to evaluate the quark propagator in the classical gluonic field found in the previous section. To this end, we consider only the zero width limit,

$$\rho=\delta(x^-)\rho(\mathbf{x}_\perp). \tag{38}$$

Beyond this limit, equations with an explicit $x^-$-dependence become much more complicated. Physically, the use of (38) in the off-forward kinematics is justified, since the light-cone fractions of the partons are small, i.e. $x,\xi\ll 1$.

The basic idea is that for $x^-\neq 0$ the field $\rho(\mathbf{x})=0$, and we have just vacuum equations; the gluon field $A_\mu$ reduces to a pure gauge. It is possible to choose the gauge in such a way that for $x^-<0$ the field disappears, $A_\mu=0$, and for $x^->0$ it is a pure gauge, $A_\mu=\frac{\mathrm{i}}{g}U\partial_\mu U^\dagger$ and thus the wave function of the quark has the form

$$\psi_{ps}(x)=\begin{cases}u_s(p)\mathrm{e}^{-\mathrm{i}px}, & x^-<0,\\ \int \mathrm{d}^4p'\delta(p^2-p'^2)\sum_{s'}C_{ss'}(p,p')u_{s'}(p')\mathrm{e}^{-\mathrm{i}px}, & x^->0,\end{cases} \tag{39}$$

where $u_s(p)$ is a free Dirac spinor, and the matrix $C_{ss'}(p,p')$ is found from the continuity at the point $x^-=0$. One subtle point is that the Dirac operator has the form

$$\mathrm{i}\hat{D}=\mathrm{i}\partial_-\gamma^-+\ldots, \tag{40}$$

and the matrix $\gamma^-$ is singular, because it is proportional to the light-cone projector $\Lambda^{(-)}$. This implies that the continuity condition must be imposed not on the function

[6] To avoid ambiguity, this is a "quenched approximation", where the diagrams with gluon loops are not taken into account. Gluon loops correspond to $\mathcal{O}(\alpha_\mathrm{s})$-corrections.

$\psi_{ps}(x)$ as a whole, as in [21, 22, 24], but rather only on the component[7] $\psi_{ps}^{(-)}(x) = \Lambda^{(-)}\psi_{ps}(x)$. The final result for the wave function is

$$\begin{aligned}\psi_{ps}(x) = {} & \theta(-x^-)u_s(p)\mathrm{e}^{-\mathrm{i}p\cdot x} + \theta(x^-)U(x_\perp) \\ & \times \int \frac{\mathrm{d}^4k}{(2\pi)^4}\delta(k^- - p^-)\delta\left(k^+ - \frac{k_\perp^2+p^2}{2p^-}\right) \\ & \times \left(\int \mathrm{d}^2z\mathrm{e}^{\mathrm{i}(p_\perp - k_\perp)\cdot z}U^\dagger(z)\right)\mathrm{e}^{-\mathrm{i}k\cdot x} \\ & \times \left(1 + \frac{\gamma_0}{k^-\sqrt{2}}(\hat{k}_\perp + M)\right)\Lambda^{(-)}u_s(p)\,, \end{aligned} \tag{41}$$

where $M$ is the mass of the quark. The evaluation of the quark propagator according to

$$S(x,y) = \int \frac{\mathrm{d}^4p}{(2\pi)^4}\frac{\sum_s \psi_{ps}(x)\bar{\psi}_{ps}(y)}{p^2 - M^2 + \mathrm{i}0}\,, \tag{42}$$

yields

$$S(x,y) - S_0(x-y) = \begin{cases} 0\,, & x^-<0\,,\ y^-<0\,, \\ (U(x_\perp)U^\dagger(y_\perp)-1)S_0(x-y)\,, & x^->0\,,\ y^->0\,, \\ \int \frac{\mathrm{d}^4p}{(2\pi)^4}\frac{1}{p^2-M^2+\mathrm{i}0}\int\frac{\mathrm{d}^2k}{(2\pi)^2} & \\ \quad\times\exp\left\{\mathrm{i}\left(\frac{k_\perp^2+M^2}{2p^-}y^- + p^-y^+ - k_\perp y_\perp - p\cdot x\right)\right\} & \\ \quad\times\int \mathrm{d}^2z\mathrm{e}^{-\mathrm{i}(p_\perp-k_\perp)z}(\hat{p}+M)\Lambda^{(+)}\left(1+\frac{\gamma_0}{p^-\sqrt{2}}(M-\hat{k}_\perp)\right) & \\ \quad\times(U(z)U^\dagger(y_\perp)-1)\,, & x^-<0\,,\ y^->0\,, \\ \int \frac{\mathrm{d}^4p}{(2\pi)^4}\frac{1}{p^2-M^2+i0}\int\frac{\mathrm{d}^2k}{(2\pi)^2} & \\ \quad\times\exp\left\{-\mathrm{i}\left(\frac{k_\perp^2+M^2}{2p^-}x^- + p^-x^+ - k_\perp x_\perp - p\cdot y\right)\right\} & \\ \quad\times\int \mathrm{d}^2z\mathrm{e}^{\mathrm{i}(p_\perp-k_\perp)z}\left(1+\frac{\gamma_0}{p^-\sqrt{2}}(\hat{k}_\perp+M)\right)\Lambda^{(-)}(\hat{p}+M) & \\ \quad\times(U(x_\perp)U^\dagger(z)-1)\,, & x^->0\,,\ y^-<0\,, \end{cases} \tag{43}$$

where $S_0(x-y)$ is the free propagator

$$S_0(x-y) = \int \frac{\mathrm{d}^4p}{(2\pi)^4}\frac{\mathrm{e}^{-\mathrm{i}p(x-y)}}{\hat{p}-M+\mathrm{i}0}\,. \tag{44}$$

It might be checked that the propagator $S(x,y)$ satisfies $(\mathrm{i}\hat{D}-M)S(x,y) = \delta(x-y)$ as well as reduces to $S_0(x-y)$ in the $U\to 1$ limit.

## 3 Unintegrated quark GPDs

In this section we evaluate the unintegrated quark GPDs defined via the following matrix element (we assume that the target has spin 0):

$$\begin{aligned} & H(x,\xi,\boldsymbol{\Delta}_\perp,\mathbf{k}_\perp) \\ & \quad = \int\frac{\mathrm{d}z^-}{2\pi}\int \mathrm{d}^2r_\perp \mathrm{e}^{-\mathrm{i}\mathbf{k}_\perp\mathbf{r}_\perp}\mathrm{e}^{\mathrm{i}x\bar{P}^+z^-} \\ & \quad\quad\times\left\langle P'\middle|\bar{\psi}\left(-\frac{z^-}{2}-\frac{\mathbf{r}_\perp}{2}\right)\gamma^+\psi\left(\frac{z^-}{2}+\frac{\mathbf{r}_\perp}{2}\right)\middle|P\right\rangle. \end{aligned} \tag{45}$$

In the forward limit ($\boldsymbol{\Delta}_\perp\to 0, \xi\to 0$) the function $H(x,\xi,\boldsymbol{\Delta}_\perp,\mathbf{k}_\perp)$ reduces to the unintegrated parton distribution $q(x,\mathbf{k}_\perp)$, and when integrated over $\mathbf{k}_\perp$, it gives ordinary GPDs. In the quasiclassical approximation, (45) reduces to

$$\begin{aligned} & H(x,\xi,\boldsymbol{\Delta}_\perp,\mathbf{k}_\perp) = \\ & \quad\int\frac{\mathrm{d}z^-}{2\pi}\mathrm{e}^{\mathrm{i}x\bar{P}^+z^-}\int\mathrm{d}^2r_\perp\mathrm{e}^{-\mathrm{i}\mathbf{k}_\perp\mathbf{r}_\perp}\mathrm{i}\bar{P}^+\int\mathrm{d}^3X\mathrm{e}^{-\mathrm{i}\boldsymbol{\Delta}\mathbf{X}} \\ & \quad\times\left\langle \mathrm{Tr}\left[\gamma^+S\left(-\frac{z^-}{2}-\frac{\mathbf{r}_\perp}{2}-\mathbf{X},\frac{z^-}{2}+\frac{\mathbf{r}_\perp}{2}-\mathbf{X}\right)\right]\right\rangle, \end{aligned} \tag{46}$$

where here and below angular brackets without explicit initial and final states $\langle\dots\rangle$ are the short-hand notation for averaging (integration) over all possible configurations $\rho(x)$, i.e. $\langle\hat{O}\rangle := \int\mathcal{D}\rho W[\rho]O(\rho)$. Substituting the propagator (43) and taking the integral over each domain, one obtains the final result

$$H(x,\xi,\boldsymbol{\Delta}_\perp,\mathbf{k}_\perp) = H^{(+-)} + H^{(-+)}\,, \tag{47}$$

where

$$\begin{aligned} & H^{+-} \\ & \quad = 2N_c\int\frac{\mathrm{d}^2\kappa^\perp}{(2\pi)^2}\tilde{\gamma}\left(\kappa^\perp+\frac{\boldsymbol{\Delta}^\perp}{2},\kappa^\perp-\frac{\boldsymbol{\Delta}^\perp}{2}\right) \\ & \quad\times\frac{M^2-\left(\mathbf{k}+\frac{\boldsymbol{\Delta}_\perp}{2}\right)\cdot(\mathbf{k}-\kappa_\perp)}{(x-\xi)((\mathbf{k}-\kappa_\perp)^2+M^2)-(x+\xi)\left(\left(\mathbf{k}+\frac{\boldsymbol{\Delta}_\perp}{2}\right)^2+M^2\right)} \\ & \quad\times\ln\left|\frac{x-\xi}{x+\xi}\frac{(\mathbf{k}-\kappa_\perp)^2+M^2}{\left(\mathbf{k}+\frac{\boldsymbol{\Delta}_\perp}{2}\right)^2+M^2}\right|, \end{aligned} \tag{48}$$

$$\begin{aligned} & H^{-+} \\ & \quad = 2N_c\int\frac{\mathrm{d}^2\kappa^\perp}{(2\pi)^2}\tilde{\gamma}\left(\kappa^\perp+\frac{\boldsymbol{\Delta}^\perp}{2},\kappa^\perp-\frac{\boldsymbol{\Delta}^\perp}{2}\right) \\ & \quad\times\frac{M^2-\left(\mathbf{k}-\frac{\boldsymbol{\Delta}}{2}\right)\cdot(\mathbf{k}_\perp-\kappa_\perp)}{(x+\xi)((\mathbf{k}_\perp-\kappa_\perp)^2+M^2)-(x-\xi)\left(\left(\mathbf{k}-\frac{\boldsymbol{\Delta}}{2}\right)^2+M^2\right)} \\ & \quad\times\ln\left|\frac{x+\xi}{x-\xi}\frac{(\mathbf{k}_\perp-\kappa_\perp)^2+M^2}{\left(\mathbf{k}-\frac{\boldsymbol{\Delta}}{2}\right)^2+M^2}\right|; \end{aligned} \tag{49}$$

the superscript signs $(\pm,\pm)$ refer to different integration domains over $(\mathrm{d}X^-,\mathrm{d}z^-)$ in (46), and function $\tilde{\gamma}(\kappa-$

[7] Thanks to P. Pobylitsa. The attempt to impose the continuity on both components $\psi_{ps}^{(+)}$ and $\psi_{ps}^{(-)}$ leads to inconsistency with the equations of motion [51].

$\frac{\boldsymbol{\Delta}_\perp}{2}, \kappa + \frac{\boldsymbol{\Delta}_\perp}{2}\Big)$ is defined as

$$\tilde{\gamma}\left(\kappa + \frac{\boldsymbol{\Delta}_\perp}{2}, \kappa - \frac{\boldsymbol{\Delta}_\perp}{2}\right) := \int \frac{\mathrm{d}^2\rho \mathrm{d}^2 X}{(2\pi)^2} \mathrm{e}^{\mathrm{i}\Delta^\perp X^\perp + \mathrm{i}\kappa^\perp \rho} \times \left\langle U^\dagger\left(X + \frac{\rho}{2}\right) U\left(X - \frac{\rho}{2}\right)\right\rangle . \tag{50}$$

Evaluation of this quantity (see Appendix B for details) yields

$$\tilde{\gamma}\left(\kappa + \frac{\boldsymbol{\Delta}_\perp}{2}, \kappa - \frac{\boldsymbol{\Delta}_\perp}{2}\right) = \int \mathrm{d}^2 r \mathrm{e}^{\mathrm{i}\kappa \mathbf{r}} \int \mathrm{d}^2 X_\perp \mathrm{e}^{\mathrm{i}\boldsymbol{\Delta}_\perp \mathbf{X}_\perp} \exp\left[-g^2 N_c \times \left(\frac{\tilde{f}\left(\mathbf{0}, \frac{\mathbf{r}}{2} - \mathbf{X}\right) + \tilde{f}\left(\mathbf{0}, -\frac{\mathbf{r}}{2} - \mathbf{X}\right)}{2} - \tilde{f}(\mathbf{r}, -\mathbf{X})\right)\right] . \tag{51}$$

Notice that GPD (47) is antisymmetric, i.e. $H(-x,\xi) = -H(-x,\xi)$. Also, (47) is not required to satisfy polynomiality since the original model is valid only for $x \ll 1$.

One of the subtle points of the result (47) is the logarithmic behaviour $\sim \ln|x \pm \xi|$ in the vicinity of the points $x \sim \pm\xi$. Physically, in these points one of the quarks has a zero light-cone fraction and becomes especially sensitive to the details of the model. However, since we are in the saturation regime, the factorization formula does not work, and we expect that such a behaviour should not cause any physical problems. In Appendix A we give details on the evaluation of (47), and in particular we discuss the logarithmic singularities.

## 4 DVCS amplitude

In this section we evaluate the DVCS amplitude directly (not using factorization). The first reason to do this is that the GPDs evaluated in the previous section are valid only for small values $x \ll 1$, whereas the convolution formula which follows from factorization implies integration over the light-cone fraction over the region $-1 < x < 1$. The second reason is that, as we discussed in Sect. 1, in the saturation (high-density) regime the convolution formula becomes invalid.

The starting point of our derivation is the definition of the DVCS amplitude

$$A_{\mu\nu} = -\mathrm{i}\int \mathrm{d}^4 z \langle P'|J_\nu(0) J_\mu(z)|P\rangle_A \mathrm{e}^{-\mathrm{i}q\cdot z} . \tag{52}$$

In the quasiclassical approximation the matrix element $\langle P'|J_\nu(0)J_\mu(z)|P\rangle_A$ is reduced to

$$\begin{aligned}\langle P'|J_\nu(0)J_\mu(z)|P\rangle_A &= \int \mathrm{d}^3 X \mathrm{e}^{\mathrm{i}\boldsymbol{\Delta}\mathbf{X}} \langle P'|J_\nu(-\mathbf{X}) J_\mu(z-\mathbf{X})|P\rangle \\ &= -\int \mathrm{d}^3 X \mathrm{e}^{\mathrm{i}\boldsymbol{\Delta}\mathbf{X}} \langle \mathrm{Tr}[\gamma_\mu S(z-\mathbf{X}, -\mathbf{X})\gamma_\nu S(-\mathbf{X}, z-\mathbf{X})]\rangle ,\end{aligned} \tag{53}$$

where $S(x,y)$ is the propagator (43). Substituting (43) into (53) and taking the integrals, we may reduce the DVCS amplitude to the form

$$\begin{aligned} A_{\mu\nu} = \mathrm{i}\frac{M_A}{2\pi} \int \frac{\mathrm{d}^3 p}{(2\pi)^3} \frac{\mathrm{d}^2 k}{(2\pi)^2} \tilde{\gamma}\left(\mathbf{k} + \frac{\boldsymbol{\Delta}_\perp}{2}, \mathbf{k} - \frac{\boldsymbol{\Delta}_\perp}{2}\right) \\ \times \frac{\Theta\left(-\frac{q^-}{2} \le p^- \le \frac{q^-}{2}\right)}{q^+((p^-)^2 - (q^-)^2/4) + \frac{k_\perp^2 + M^2}{2} q^- - \mathrm{i}0} \\ \times \Big[2(q^+ - \Delta^+)((p^-)^2 - (q^-)^2/4) + p^- \mathbf{p}_\perp \boldsymbol{\Delta}_\perp \\ + q^-\left(\mathbf{p}_\perp^2 + M^2 + \frac{\boldsymbol{\Delta}_\perp^2}{4}\right)\Big]^{-1} \\ \times \left(8N_c \delta_{\mu+}\delta_{\nu+}(M^2 - \mathbf{k}_\perp^2 - \mathbf{p}_\perp^2)\left(M^2 - \mathbf{p}_\perp^2 + \frac{\boldsymbol{\Delta}_\perp^2}{4}\right)\right. \\ + 8N_c \delta_{\mu\perp}\delta_{\nu\perp}[\mathbf{p}_\perp^\mu \mathbf{p}_\perp^\nu ((q^-)^2 - 4(p^-)^2) + \\ + p^- g_{\mu\nu}(4p^-(M^2 + \mathbf{p}_\perp^2) - q^- \mathbf{p}_\perp \cdot \boldsymbol{\Delta}_\perp)] \\ + 32N_c \delta_{\mu-}\delta_{\nu-}\left((p^-)^2 - \frac{(q^-)^2}{4}\right)^2 \\ + 8N_c(\delta_{\mu+}\delta_{\nu-} + \delta_{\nu+}\delta_{\mu-})\left((p^-)^2 - \frac{(q^-)^2}{4}\right) \\ \left. \times \left(2M^2 - 2\mathbf{p}_\perp^2 - \mathbf{k}_\perp^2 + \frac{\boldsymbol{\Delta}_\perp^2}{4}\right)\right) . \end{aligned} \tag{54}$$

One interesting point is that the real part of (54) is *exactly* zero. Indeed, taking the imaginary part of the first ratio containing $-\mathrm{i}0$ and using

$$\frac{1}{x - \mathrm{i}0} = P\left(\frac{1}{x}\right) + \mathrm{i}\pi\delta(x) , \tag{55}$$

we can immediately find that the argument of the $\delta$-function is zero only for

$$|p^-| = \frac{q^-}{2}\sqrt{1 + \frac{2(k_\perp^2 + M^2)}{Q^2}} \ge \frac{q^-}{2} , \tag{56}$$

i.e. outside the integration domain. For comparison, from phenomenology it is known that the high-energy amplitude gets a dominant contribution from the imaginary part.

## 5 Results for GPDs and DVCS cross sections

In this section we present results of the numerical evaluation of the GPDs and DVCS cross sections. In Sect. 5.1 we consider first the results with a simpler parameterization (10), and after that in Sect. 5.2 with a more realistic parameterization (9).

### 5.1 Results with parameterization II

As one can see from (29), for both parameterizations I and II the $x$-dependence of the gluon GPD $H_A^g(x,\xi,t)$

is trivial – just $1/x$ for all $(\xi, t)$. For the quark GPDs $H_A^q(x,\xi,t)$ the $x$-dependence is more complicated; however, in the forward case the parton distribution $q_A(x)$ also has a simple $1/x$-dependence. For better understanding, we prefer to discuss the results for the gluons in terms of the ratio $H_A^g(x,\xi,t)/g_A(x)$, which measures the off-forward effects, and $g_A(x)$ is the forward gluon PDF evaluated in the same model.

In Fig. 2 we plot the $\xi$- and $t$-dependence of the ratio $H_A^g(x,\xi,t)/g_A(x)$ for different nuclei. In the upper panel of Fig. 2 we plot the $t$-dependence of the ratio $H_A^g(x,\xi,t)/g_A(x)$ in the nuclei for $\xi = 0$. We can see that $H^g(x,\xi,t)$ is decreasing as a function of $t$. For the sake of comparison, on the same plot we also plotted in grey lines the nuclear form factors in conventional exponential parameterization, $F_A(t) = \exp\left(\frac{R_A^2}{6}t\right)$, and for radius $R_A$ we used $R_A = 1.2\,\mathrm{fm} \times A^{1/3}$. We can see that to a good extent the $t$-dependence of the GPDs is similar to that of the form factors.

In the lower panel of Fig. 2 we plot the $\xi$-dependence of the gluon GPDs in nuclei. We can see that in the small-$\xi$ region $H^g(x,\xi,t)$ is independent of the skewedness $\xi$. This result is quite easy to understand: in the ultrarelativistic limit the nucleus in the laboratory frame is squeezed to an infinitely thin "pancake", so the condensate distribution along the $x^-$-axis is strongly peaked around $x^- \approx 0$, $\lambda_A(x^-) \sim \delta(x^-)$. As a consequence, the gluon GPD which is proportional to the Fourier transform of $\lambda_A(x^-)$, almost does not depend on $\Delta^+ \sim \xi$. The only exception is the region of sufficiently large $\xi \sim 0.1$, where the $\xi$-dependence is mainly a kinematical effect – the increase of $H^g(x,\xi,t)$ is due to decreasing $\Delta_\perp$ at fixed $t$. However, these values of $\xi \sim 0.1$ are too large, and our extrapolation of the model becomes unreliable.

In Fig. 3 we plot the $x$-, $\xi$- and $t$-dependence of the quark GPD $H_A^q(x,\xi,t)$ in nuclei. As one can see from (47), in the forward limit the quark distributions have a very simple $x$-dependence, $H_A^q(x,0,0) \equiv q_A(x) \sim 1/x$. For better legibility, we prefer to discuss results for the quarks in terms of the ratio $H_A^q(x,\xi,t)/q_A(x)$, which measures off-forward effects.

From the upper panel in Fig. 3 we can see that for $x \ll \xi$ the GPD $H_A^q(x,\xi,t)$ is decreasing approximately as $H_A^q(x,\xi,t) \sim x$, and as a result the ratio $H_A^q(x,\xi,t)/q_A(x)$ behaves approximately as $H_A^q(x,\xi,t)/q_A(x) \sim x^2$. For $x \gg \xi$, $H_A^q(x,\xi,t) \approx q_A(x)F_A(t)$, and the ratio is a constant. In the point $x = \xi$ we have a singularity $\sim \ln|x-\xi|$, which was mentioned at the end of Sect. 3 and discussed in detail in Appendix A.

From the middle panel in Fig. 3 we can see that as a function of $\xi$ the generalized quark distribution is a constant for $\xi \ll x$, but it is a decreasing function for $\xi \gg x$.

From the lower panel in Fig. 3 we can see the $t$-dependence of the GPD $H_A^q(x,\xi,t)$. For the sake of comparison, on the same plot we also plotted in grey lines the nuclear form factors in the frequently used exponential parameterization, $F_A(t) = \exp\left(\frac{R_A^2}{6}t\right)$. We can see that $H_A^q(x,\xi,t)$ is decreasing a bit faster than $F_A(t)$.

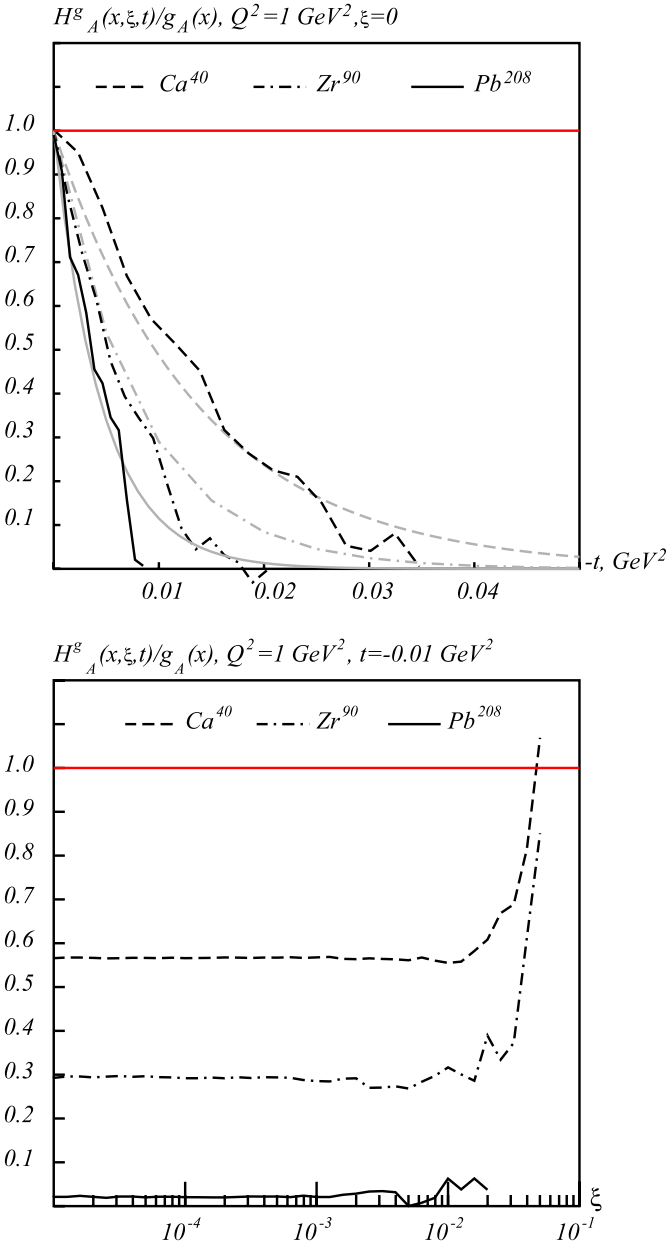


**Fig. 2.** *Upper plot*: $t$-dependence of the gluon distribution for different nuclei. $\xi = 0$, $Q^2 = 1\,\mathrm{GeV}^2$. For comparison, we also plotted in *grey lines* the nuclear form factor in the simplest exponential parameterization $F_A(t) = \exp\left(\frac{R_A^2}{6}t\right)$. *Lower plot*: $\xi$-dependence for the same nuclei for fixed $t = -0.01\,\mathrm{GeV}^2$, $Q^2 = 1\,\mathrm{GeV}^2$. We do not plot the $x$-dependence of the gluon GPD $H^g$, which is according to (29) just a trivial $1/x$ for all $(\xi, t)$

In Fig. 4 we plot the $\xi$- and $t$-dependence of the differential DVCS cross section $\mathrm{d}\sigma/\mathrm{d}t$ for fixed $Q^2$ and different nuclei.

From the upper part of Fig. 4 we can see that the cross section is growing when $\xi$ is decreasing, but at some $\xi$, which we call $\xi_{\mathrm{sat}}(Q^2, A)$, we have a qualitative transition to the saturation. The value $\xi_{\mathrm{sat}}(Q^2, A)$ depends on the external kinematics. The relatively large value $\xi_{\mathrm{sat}} \sim 0.01$ is

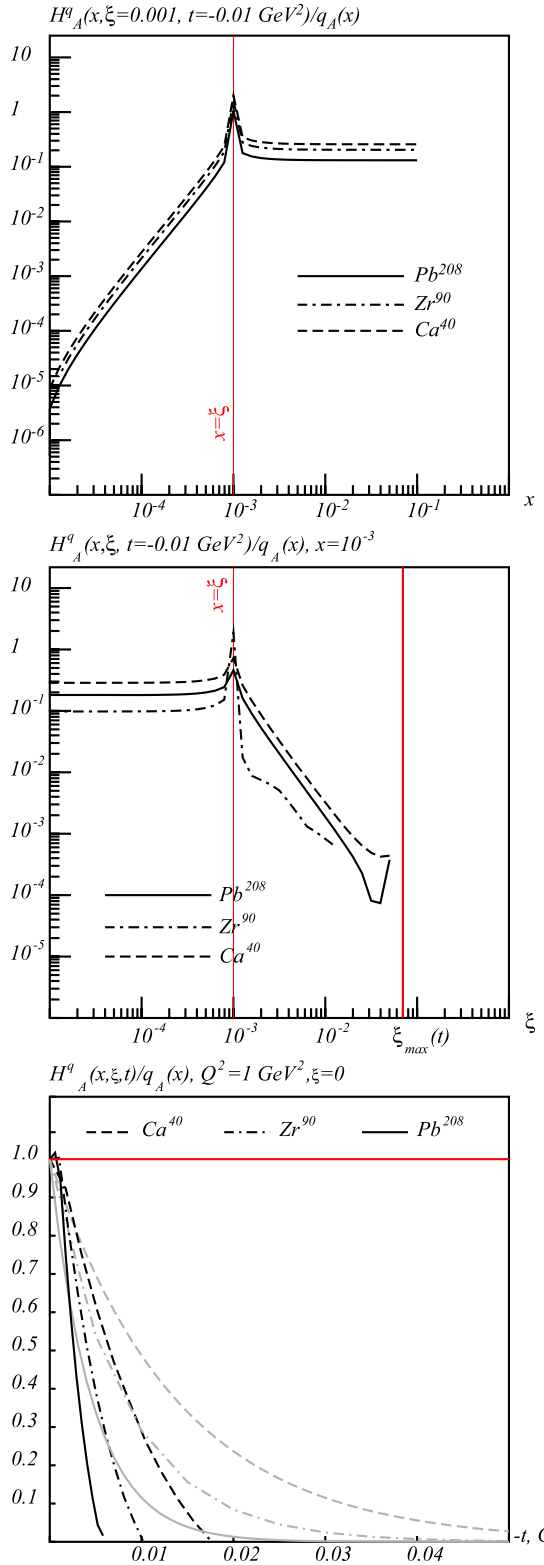


**Fig. 3.** *Upper plot*: $x$-dependence of the quark GPD $H_A(x,\xi,t)$. $\xi = 10^{-2}$, $Q^2 = 1\,\mathrm{GeV}^2$. *Middle plot*: $\xi$-dependence of the same GPD $H_A(x,\xi,t)$ for fixed $x = 10^{-4}$, $Q^2 = 1\,\mathrm{GeV}^2$, $\xi_{\max} = \sqrt{-t/(4M^2 - t)}$. *Lower plot*: $t$-dependence of the same GPD $H_A(x,\xi,t)$. For comparison, we also plotted in *grey lines* the nuclear form factor in the the simplest exponential parameterization $F_A(t) = \exp\left(\frac{R_A^2}{6}t\right)$

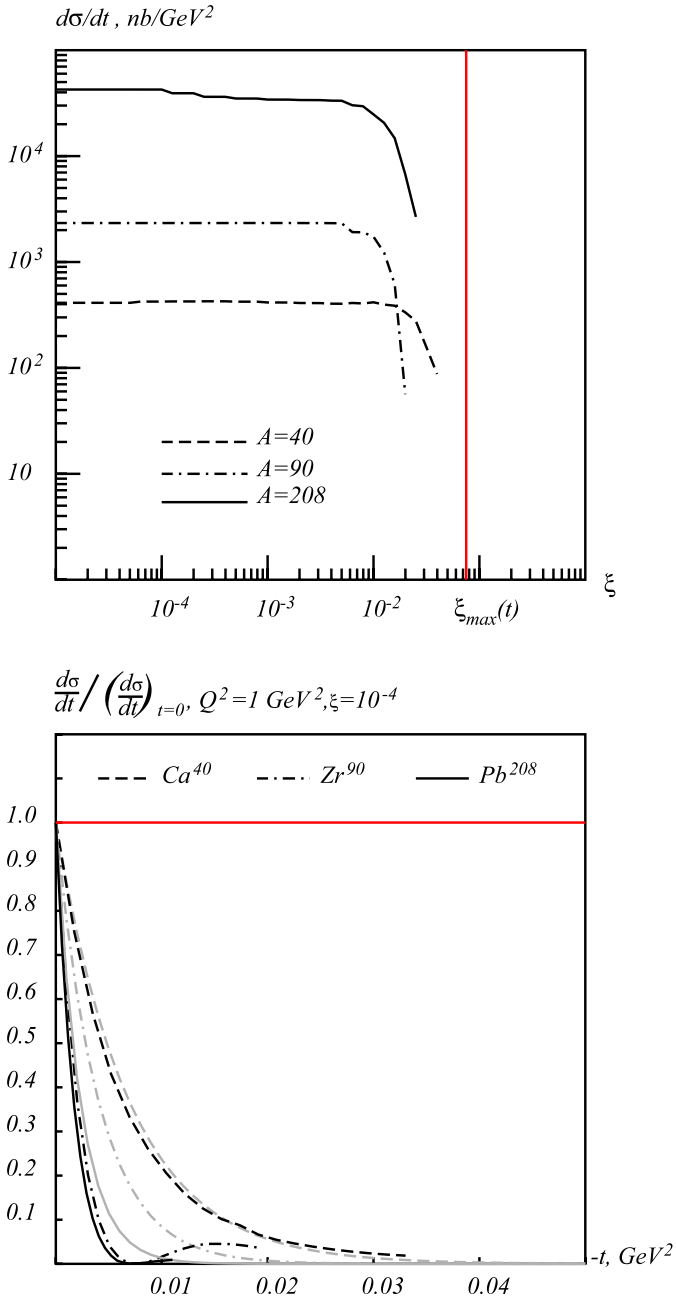


**Fig. 4.** *Upper plot*: $\xi$-dependence of the differential DVCS cross section in the CGC model for different nuclei. Kinematic is chosen as $Q^2 = 1\,\mathrm{GeV}^2$, $t = -0.01\,\mathrm{GeV}^2$. *Lower plot*: $t$-dependence of the DVCS cross section at fixed $\xi = 10^{-4}$. On the *lower plot*, we also plotted in *grey lines* what one would have with the simplest factorized $t$-dependence of the DVCS amplitude and exponential parameterization for the form factor: $\frac{\mathrm{d}\sigma}{\mathrm{d}t} \sim F_A^2(t) \sim \exp\left(\frac{R_A^2}{3}t\right)$

due to the small value of $Q^2 = 1\,\mathrm{GeV}^2$, $\xi_{\mathrm{sat}}$ is decreasing when $Q^2$ increases.

From the lower plot on Fig. 4 we can see the $t$-dependence of the differential cross section $\mathrm{d}\sigma/\mathrm{d}t$. For the sake of comparison, on the same plot we also plotted in grey lines the nuclear form factors in a conventional exponential

parameterization, $F_A(t) = \exp\left(\frac{R_A^2}{6}t\right)$. We see that $\mathrm{d}\sigma/\mathrm{d}t$ is decreasing a bit faster than $F_A^2(t)$.

### 5.2 Results with parameterization I

In this section we discuss the results of a color glass condensate model in the parameterization (9). The crucial point is that this model explicitly contains the saturation scale $Q_s^2$,

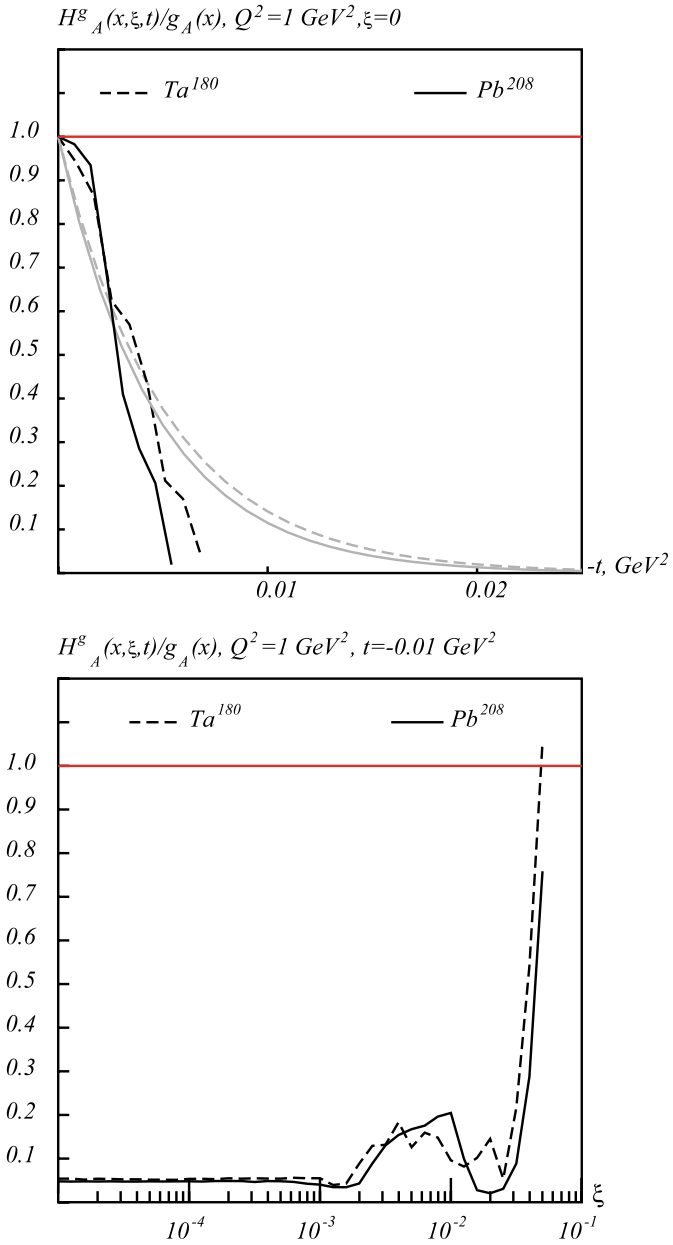


**Fig. 5.** *Upper plot*: $t$-dependence of the gluon distribution for different nuclei. $\xi = 0$, $Q^2 = 1\,\mathrm{GeV}^2$. *Lower plot*: $\xi$-dependence for the same nuclei for fixed $t = -0.01\,\mathrm{GeV}^2$, $Q^2 = 1\,\mathrm{GeV}^2$. We do not plot the $x$-dependence of the gluon GPD $H^g$, which is according to (29) just a trivial $1/x$ for all $(\xi, t)$. On the *upper plot*, we also plotted in *grey lines* the nuclear form factor in the simplest exponential parameterization $F_A(t) = \exp\left(\frac{R_A^2}{6}t\right)$

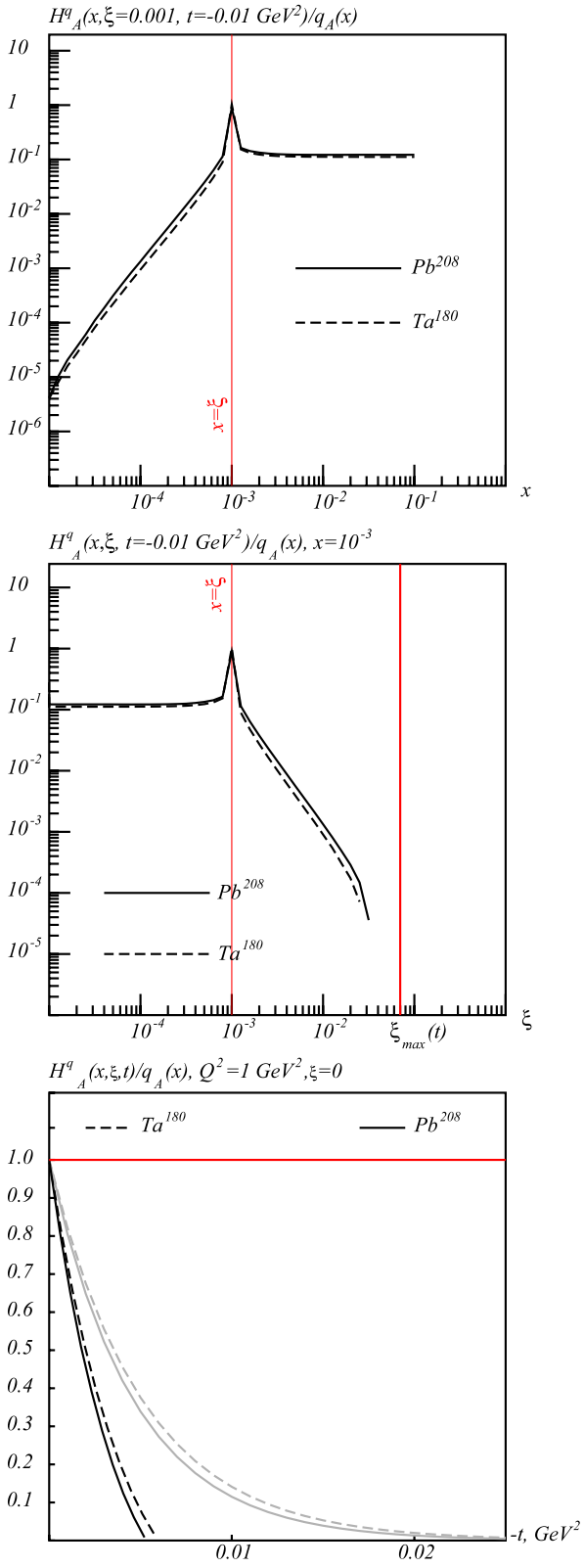


**Fig. 6.** *Upper plot*: $x$-dependence of the quark GPD $H_A(x, \xi, t)$. $\xi = 10^{-3}$, $Q^2 = 1\,\mathrm{GeV}^2$. *Middle plot*: $\xi$-dependence of the same GPD $H_A(x, \xi, t)$ for fixed $x = 10^{-3}$, $Q^2 = 1\,\mathrm{GeV}^2$. *Lower plot*: $t$-dependence of the same GPD $H_A(x, \xi, t)$. On the *upper plot*, we also plotted in *grey lines* the nuclear form factor in the simplest exponential parameterization $F_A(t) = \exp\left(\frac{R_A^2}{6}t\right)$

and as a consequence we can apply it only to the kinematics where saturation is present. In our evaluations we used for $Q_s^2$ the parameterization from [25], where $Q_s^2(A)$ is found as a solution of

$$Q_s^2(A) = \alpha_s(Q^2) N_c \mu_A^2 \ln\left(\frac{Q_s^2(A)}{\Lambda_{\rm QCD}^2}\right). \qquad (57)$$

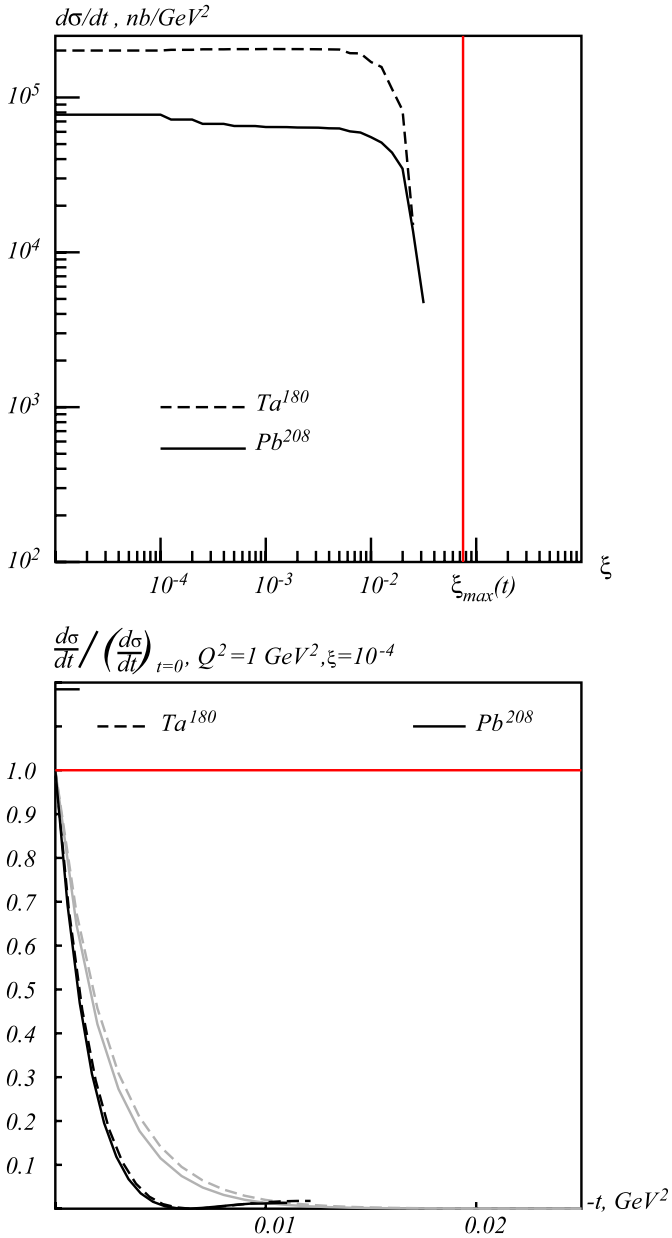


**Fig. 7.** *Upper plot*: $\xi$-dependence of the differential DVCS cross section in the CGC model for different nuclei. The kinematics is chosen as $Q^2 = 1\,\mathrm{GeV}^2$, $t = -0.01\,\mathrm{GeV}^2$. *Lower plot*: $t$-dependence of the DVCS cross section at fixed $\xi = 10^{-4}$. On the *lower plot*, we also plotted in *grey lines* what one would have with the simplest factorized $t$-dependence of the DVCS amplitude and exponential parameterization for the form factor: $\frac{\mathrm{d}\sigma}{\mathrm{d}t} \sim F_A^2(t) \sim \exp\left(\frac{R_A^2}{3} t\right)$

This equation has real solutions only for $A \gtrsim A_{\rm min}(Q^2) \sim 150$ for $Q^2 \sim 1\,\mathrm{GeV}^2$, and $A_{\rm min}(Q^2)$ is a growing function of $Q^2$.

In Figs. 5 and 6 we plot the $\xi$- and $t$-dependence of the gluon and quark distributions $H_A(x,\xi,t)/q_A(x)$, and in Fig. 7 we plot the $\xi$- and $t$-dependence of the differential DVCS cross section $\mathrm{d}\sigma/\mathrm{d}t$. We can see that qualitatively the behaviour is the same as in the previous section, although absolute values differ.

### 5.3 Comparison to DVCS cross section in GVMD model

In Fig. 8 we compare predictions for the DVCS cross section with our earlier result [19] obtained in generalized vector dominance model (GVMD). We can see the difference in the predictions of the GVMD and CGC models: in contrast to the saturation behavior in CGC, the GVMD cross section is slowly growing as $\xi^{-\alpha}$ when $\xi$ is decreasing. Nevertheless, in the region $10^{-5} \le \xi \le 10^{-3}$ predictions of both models have comparable values.

## 6 Conclusion

In this paper we considered generalized parton distributions (GPDs) and deeply virtual Compton scattering (DVCS) amplitudes in the color glass condensate model.

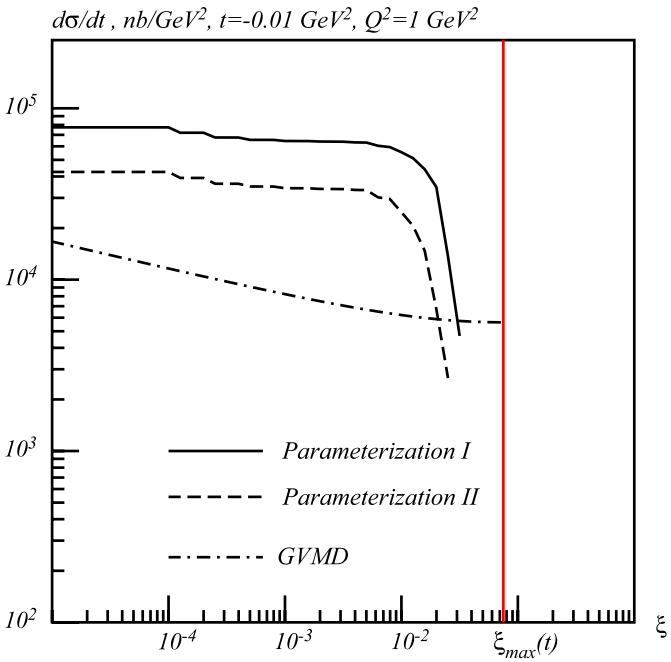


**Fig. 8.** Comparison of the $\xi$-dependence of the DVCS cross section in different models. *Solid curve* corresponds to parameterization I from (9), *dashed curve* corresponds to parameterization II from (10), *dot-dashed* corresponds to generalized vector meson dominance (GVMD) from [19]. The kinematics is chosen as $Q^2 = 1\,\mathrm{GeV}^2$, $t = -0.01\,\mathrm{GeV}^2$; for the nucleus $A = 208$ (lead)

We modified the original formulation of [21, 22] to off-forward kinematics of hard exclusive reactions, which provided the necessary framework for the calculation of GPDs and the DVCS amplitude.

We evaluated the quark and gluon GPDs in this model and studied their dependence on the variables $x$, $\xi$ and $t$. We found that the gluon GPD $H^g$ in this model has a simple $x$-dependence $H^g(x) \sim 1/x$ for all $(\xi, t)$. A similar $1/x$-behaviour was observed for the quark GPDs $H^q$ in the $x \gg \xi$ region and in the forward limit ($t = 0$). Both the quark and gluon GPDs are decreasing as a function of momentum transfer $t$, and the quark GPD is decreasing a bit faster than the gluon GPD.

Without assuming the validity of the collinear factorization, we evaluated the DVCS cross sections in the small-$\xi$ region on the large nuclei. We found that in this region the DVCS cross sections are almost independent of $\xi$. This is a manifestation of the general saturation property inherent to the CGC model. As far as absolute values are concerned, we found that the predictions of CGC in the relevant range of $\xi$ are comparable with predictions of other models, e.g. GVMD. Currently there are no experimental data available for the DVCS cross section in this kinematics.

The present calculation should be important for a wide range of future experiments. For example, gluon GPDs in the small-$x$ region may be used for the evaluation of heavy vector meson production in ultraperipheral collisions at the LHC [52, 53].

*Acknowledgements.* We would like to thank P. Pobylitsa and M. Strikman for useful discussions. The work has been partially supported by the Collaborative Research Center Bonn–Bochum–Giessen of the DFG, by the I3HP European Project (6-th Framework), by the Verbundforschung "Hadrons and Nuclei" of the BMBF, by the Graduate College Dortmund–Bochum of the DFG, by the COSY-Project Juelich, and by the AvH-Kovalevskaja Funds (M. Polyakov).



## Appendix A: Details of evaluation of (46)

In this section we evaluate the unintegrated GPD (45), which in a quasiclassical approximation was reduced to

$$\begin{aligned} H(x,\xi,\boldsymbol{\Delta}_\perp,\mathbf{k}_\perp) &= \mathrm{i}\bar{P}^+ \int \frac{\mathrm{d}z^-}{2\pi} \int \mathrm{d}^2 r_\perp \mathrm{e}^{-\mathrm{i}\mathbf{k}_\perp \mathbf{r}_\perp} \int \mathrm{d}^3 X \mathrm{e}^{-\mathrm{i}\boldsymbol{\Delta}\mathbf{X}} \\ &\times \left\langle \mathrm{Tr}\left[\gamma^+ S\left(-\frac{z^-}{2} - \frac{\mathbf{r}_\perp}{2} - \mathbf{X}, \frac{z^-}{2} + \frac{\mathbf{r}_\perp}{2} - \mathbf{X}\right)\right]\right\rangle \\ &= \mathrm{i}\bar{P}^+ \int \frac{\mathrm{d}^3\xi_1}{(2\pi)^3} \frac{\mathrm{d}^3\xi_2}{(2\pi)^3} \mathrm{e}^{\mathrm{i}p_2\cdot\xi_2 - \mathrm{i}p_1\cdot\xi_1} \langle \mathrm{Tr}[\gamma^+ S(\xi_1;\xi_2)]\rangle\,, \end{aligned} \tag{A.1}$$

where we changed the integration variables according to

$$\xi_1 = -\frac{z^-}{2} - \frac{\mathbf{r}_\perp}{2} - \mathbf{X}\,, \tag{A.2}$$

$$\xi_2 = \frac{z^-}{2} + \frac{\mathbf{r}_\perp}{2} - \mathbf{X}\,, \tag{A.3}$$

and we introduced the short-hand notation

$$\mathbf{p}_1 = x\bar{P}^+ + \mathbf{k}_\perp - \frac{\boldsymbol{\Delta}}{2}\,, \tag{A.4}$$

$$\mathbf{p}_2 = x\bar{P}^+ + \mathbf{k}_\perp + \frac{\boldsymbol{\Delta}}{2}\,. \tag{A.5}$$

Now we have to separately consider the first case $\xi_1^- > 0$, $\xi_2^- < 0$ and the second case $\xi_1^- < 0$, $\xi_2^- > 0$. All the other regions are just the vacuum contributions $\sim \delta^2(\Delta_\perp)$ and must be omitted. For the sake of brevity we will refer to the contribution of the first region as $H^{+-}$, and to the second one as $H^{-+}$.

For $\theta$-functions of the arguments $\pm\xi_{1,2}$, we will use the integral representation

$$\theta(\pm\xi) = \frac{1}{2\pi\mathrm{i}} \int_{-\infty}^{\infty} \mathrm{d}\alpha \frac{\mathrm{e}^{\pm\mathrm{i}\alpha\xi}}{\alpha - i0} = -\frac{1}{2\pi\mathrm{i}} \int_{-\infty}^{\infty} \mathrm{d}\alpha \frac{\mathrm{e}^{\mp\mathrm{i}\alpha\xi}}{\alpha + \mathrm{i}0}\,. \tag{A.6}$$

### A.1 Evaluation of $H^{+-}$

In the first case we have explicitly

$$\begin{aligned} H^{+-} &= -\mathrm{i}\bar{P}^+ \int \frac{\mathrm{d}^3\xi_1}{(2\pi)^3} \frac{\mathrm{d}^3\xi_2}{(2\pi)^3} \mathrm{e}^{\mathrm{i}p_2\cdot\xi_2 - \mathrm{i}p_1\cdot\xi_1} \\ &\times \int \frac{\mathrm{d}\alpha_1\,\mathrm{d}\alpha_2}{(2\pi)^2} \frac{\mathrm{e}^{\mathrm{i}(\alpha_1\xi_1^- - \alpha_2\xi_2^-)}}{(\alpha_1 - \mathrm{i}0)(\alpha_2 - \mathrm{i}0)} \\ &\times \int \frac{\mathrm{d}^4 p}{(2\pi)^4} \frac{1}{p^2 - M^2 + \mathrm{i}0} \int \frac{\mathrm{d}^2 q}{(2\pi)^2} \\ &\times \exp\left\{-\mathrm{i}\left(\frac{q_\perp^2 + M^2}{2p^-}\xi_1^- - q_\perp\cdot\xi_{1\perp} - p^+\xi_2^- + \mathbf{p}_\perp\xi_2^\perp\right)\right\} \\ &\times \int \mathrm{d}^2 z \mathrm{e}^{\mathrm{i}(p_\perp - q_\perp)z} \langle U^\dagger(z) U(\xi_{1\perp})\rangle \\ &\times \mathrm{Tr}\left[\gamma_+\left(1 + \frac{\gamma_0}{p^-\sqrt{2}}(\hat{q}_\perp + M)\right)\Lambda^{(-)}(\hat{p} + M)\right]. \end{aligned} \tag{A.7}$$

Now we evaluate each of the integrals:

$$\begin{aligned} &\int \frac{\mathrm{d}\xi_1^-\,\mathrm{d}\xi_2^-}{(2\pi)^2} \mathrm{e}^{\mathrm{i}p_1^+\xi_1^- - ip_2^+\xi_2^-} \mathrm{e}^{\mathrm{i}(\alpha_1\xi_1^- - \alpha_2\xi_2^-)} \\ &\quad\times \exp\left(-\mathrm{i}\frac{q_\perp^2 + M^2}{2p^-}\xi_1^- + \mathrm{i}p^+\xi_2^-\right) \\ &= \delta\left(\alpha_1 + p_1^+ - \frac{q_\perp^2 + M^2}{2p^-}\right)\delta(\alpha_2 + p_2^+ - p^+)\,, \\ &\quad\times \int \frac{\mathrm{d}^2 p_\perp}{(2\pi)^2} \int \mathrm{d}^2 z \mathrm{e}^{\mathrm{i}(p_\perp - q_\perp)z} \int \frac{\mathrm{d}^2\xi_1^\perp\,\mathrm{d}^2\xi_2^\perp}{(2\pi)^4} \\ &\quad\times \mathrm{e}^{-\mathrm{i}p_1^\perp\xi_1^\perp + \mathrm{i}p_2^\perp\xi_2^\perp} \mathrm{e}^{\mathrm{i}q_\perp\xi_1^\perp - \mathrm{i}p_\perp\xi_2^\perp} \langle U(\xi_{1\perp}) U^\dagger(z)\rangle \end{aligned} \tag{A.8}$$

$$= \int \mathrm{d}^2 z \mathrm{e}^{\mathrm{i}(p_{2\perp}-q_\perp)z} \times \int \frac{\mathrm{d}^2\xi_1^\perp}{(2\pi)^2} \mathrm{e}^{-\mathrm{i}(p_1^\perp - q_\perp)\xi_1^\perp} \langle U^\dagger(z) U(\xi_{1\perp})\rangle \Big|_{p_\perp = p_{2\perp}} . \tag{A.9}$$

Now we change the dummy integration variables $\xi_1^\perp$ and $\mathbf{z}$ to $\mathbf{X}^\perp$ and $\rho^\perp$:

$$\xi_1^\perp := X^\perp - \frac{\rho^\perp}{2}\,, \tag{A.10}$$

$$z := X^\perp + \frac{\rho^\perp}{2}\,,$$

$$\Longrightarrow \quad \int \mathrm{d}^2 z \mathrm{e}^{\mathrm{i}(p_{2\perp}-q_\perp)z} \int \frac{\mathrm{d}^2\xi_1^\perp \mathrm{d}^2\xi_2^\perp}{(2\pi)^4} \mathrm{e}^{-\mathrm{i}p_1^\perp\xi_1^\perp + \mathrm{i}p_2^\perp\xi_2^\perp} \times \mathrm{e}^{\mathrm{i}q_\perp\xi_1^\perp - \mathrm{i}p_{2\perp}\xi_2^\perp} \langle U(\xi_{1\perp}) U^\dagger(z)\rangle = \tilde\gamma\left(k^\perp - q^\perp + \frac{\Delta^\perp}{2}, k^\perp - q^\perp - \frac{\Delta^\perp}{2}\right), \tag{A.11}$$

where $\tilde\gamma$ was defined in (50). It is convenient to make a shift of the dummy integration variable according to

$$\int \frac{\mathrm{d}^2 q^\perp}{(2\pi)^2} \to \int \frac{\mathrm{d}^2\kappa^\perp}{(2\pi)^2}\,, \quad \kappa^\perp = \mathbf{k}^\perp - \mathbf{q}^\perp\,. \tag{A.12}$$

$$\Longrightarrow \quad H^{+-}(x,\xi,t,k_\perp) = -\mathrm{i}N_c \int \frac{\mathrm{d}^2\kappa^\perp}{(2\pi)^2} \tilde\gamma\left(\kappa^\perp + \frac{\Delta^\perp}{2}, \kappa^\perp - \frac{\Delta^\perp}{2}\right) \times \int \frac{\mathrm{d}p^+\mathrm{d}p^-}{(2\pi)^2} \frac{1}{2p^+p^- - p_2^{\perp 2} - M^2 + \mathrm{i}0} \times \frac{1}{p^+ - p_2^+ - \mathrm{i}0} \frac{1}{\frac{(k_\perp-\kappa_\perp)^2+M^2}{2p^-} - p_1^+ - \mathrm{i}0} \times \frac{M^2 - \mathbf{p}_{2\perp}(\mathbf{k}_\perp - \kappa_\perp)}{p^-}\,. \tag{A.13}$$

Now we take the integrals over $p^+$ and $p^-$ in (A.13). The first integral is taken over $p^+$, and the result is

$$\int \frac{\mathrm{d}p^+}{(2\pi)} \frac{1}{2p^+p^- - p_2^{\perp 2} - M^2 + \mathrm{i}0} \frac{1}{p^+ - p_2^+ - \mathrm{i}0} = \frac{\mathrm{i}\theta(p^-)}{2p_2^+p^- - (p_2^\perp)^2 - M^2 + \mathrm{i}0}\,. \tag{A.14}$$

Integration over $p^-$ yields

$$H^{+-}(x,\xi,t,k_\perp) = 2N_c \int \frac{\mathrm{d}^2\kappa^\perp}{(2\pi)^2} \tilde\gamma\left(\kappa^\perp + \frac{\Delta^\perp}{2}, \kappa^\perp - \frac{\Delta^\perp}{2}\right) \times \frac{M^2 - \mathbf{p}_{2\perp}\cdot(\mathbf{k}_\perp - \kappa_\perp)}{(x-\xi)((\mathbf{k}_\perp-\kappa_\perp)^2 + M^2) - (x+\xi)(p_2^{\perp 2} + M^2)} \times \ln\left|\frac{x-\xi}{x+\xi}\frac{((\mathbf{k}_\perp-\kappa_\perp)^2+M^2)}{(p_2^{\perp 2}+M^2)}\right|$$

$$= 2N_c \int \frac{\mathrm{d}^2\kappa^\perp}{(2\pi)^2} \tilde\gamma\left(\kappa^\perp + \frac{\Delta^\perp}{2}, \kappa^\perp - \frac{\Delta^\perp}{2}\right) \times \frac{M^2 - \left(\mathbf{k} + \frac{\boldsymbol{\Delta}_\perp}{2}\right)\cdot(\mathbf{k}-\kappa_\perp)}{(x-\xi)((\mathbf{k}-\kappa_\perp)^2+M^2) - (x+\xi)\left(\left(\mathbf{k}+\frac{\boldsymbol{\Delta}_\perp}{2}\right)^2 + M^2\right)} \times \ln\left|\frac{x-\xi}{x+\xi}\frac{(\mathbf{k}-\kappa_\perp)^2+M^2}{\left(\mathbf{k}+\frac{\boldsymbol{\Delta}_\perp}{2}\right)^2+M^2}\right|. \tag{A.15}$$

## A.2 Evaluation of $H^{-+}$

In complete analogy we evaluate the term $H^{-+}$:

$$H^{-+} = -\mathrm{i}\int \frac{\mathrm{d}^3\xi_1}{(2\pi)^3}\frac{\mathrm{d}^3\xi_2}{(2\pi)^3} \mathrm{e}^{\mathrm{i}p_2\cdot\xi_2 - \mathrm{i}p_1\cdot\xi_1} \times \int \frac{\mathrm{d}\alpha_1\,\mathrm{d}\alpha_2}{(2\pi)^2} \frac{\mathrm{e}^{\mathrm{i}(\alpha_1\xi_1^- - \alpha_2\xi_2^-)}}{(\alpha_1+\mathrm{i}0)(\alpha_2+\mathrm{i}0)} \times \int \frac{\mathrm{d}^4 p}{(2\pi)^4} \frac{1}{p^2 - M^2 + \mathrm{i}0} \int \frac{\mathrm{d}^2 q}{(2\pi)^2} \times \exp\left\{\mathrm{i}\left(\frac{q_\perp^2 + M^2}{2p^-}\xi_2^- - q_\perp\cdot\xi_{2\perp} - p^+\xi_1^- + \mathbf{p}_\perp\xi_1^\perp\right)\right\} \times \int \mathrm{d}^2 z \mathrm{e}^{-\mathrm{i}(p_\perp - q_\perp)z} \langle U^\dagger(\xi_2^\perp) U(z)\rangle \times \mathrm{Tr}\left[\gamma_+(\hat p + M)\Lambda^{(+)}\left(1 + \frac{\gamma_0}{p^-\sqrt{2}}(M - \hat k_\perp)\right)\right]. \tag{A.16}$$

Now take the integrals term-by-term in complete analogy with the previous case:

$$\int \frac{\mathrm{d}\xi_1^-\,\mathrm{d}\xi_2^-}{(2\pi)^2} \mathrm{e}^{\mathrm{i}p_1^+\xi_1^- - \mathrm{i}p_2^+\xi_2^-} \mathrm{e}^{\mathrm{i}(\alpha_1\xi_1^- - \alpha_2\xi_2^-)} \times \exp\left(\mathrm{i}\frac{q_\perp^2 + M^2}{2p^-}\xi_2^- - \mathrm{i}p^+\xi_1^-\right) = \delta(\alpha_1 + p_1^+ - p^+)\delta\left(\alpha_2 + p_2^+ - \frac{q_\perp^2 + M^2}{2p^-}\right), \times \int \frac{\mathrm{d}^2 p_\perp}{(2\pi)^2} \int \mathrm{d}^2 z \mathrm{e}^{-\mathrm{i}(p_\perp - q_\perp)z} \int \frac{\mathrm{d}^2\xi_1^\perp\,\mathrm{d}^2\xi_2^\perp}{(2\pi)^4} \times \mathrm{e}^{-\mathrm{i}p_1^\perp\xi_1^\perp + \mathrm{i}p_2^\perp\xi_2^\perp} \mathrm{e}^{-\mathrm{i}q_\perp\xi_2^\perp + \mathrm{i}p_\perp\xi_1^\perp} \langle U^\dagger(\xi_2^\perp) U(z)\rangle = \int \mathrm{d}^2 z \mathrm{e}^{-\mathrm{i}(p_{1\perp} - q_\perp)z} \times \int \frac{\mathrm{d}^2\xi_2^\perp}{(2\pi)^2} \mathrm{e}^{\mathrm{i}(p_2^\perp - q_\perp)\xi_2^\perp} \langle U^\dagger(\xi_{2\perp}) U(z)\rangle \Big|_{p_\perp = p_{1\perp}} . \tag{A.17}$$

Now change the dummy integration variables $\xi_2^\perp, \mathbf{z}$ to $\mathbf{X}, \rho^\perp$ according to

$$\xi_2^\perp := X^\perp + \frac{\rho^\perp}{2}\,, \tag{A.18}$$

$$z := X^\perp - \frac{\rho^\perp}{2} \tag{A.19}$$

$$\begin{aligned}\Longrightarrow\quad & \int \frac{\mathrm{d}^2 p_\perp}{(2\pi)^2} \int \mathrm{d}^2 z \mathrm{e}^{-\mathrm{i}(p_\perp - q_\perp)z} \int \frac{\mathrm{d}^2\xi_1^\perp\, \mathrm{d}^2\xi_2^\perp}{(2\pi)^4} \\ & \times \mathrm{e}^{-\mathrm{i}p_1^\perp \xi_1^\perp + \mathrm{i}p_2^\perp \xi_2^\perp} \mathrm{e}^{-\mathrm{i}q_\perp \xi_2^\perp + \mathrm{i}p_\perp \xi_1^\perp} \langle U^\dagger(\xi_2^\perp) U(z)\rangle \\ & = \tilde\gamma\left(k^\perp - q^\perp + \frac{\Delta^\perp}{2}, k^\perp - q^\perp - \frac{\Delta^\perp}{2}\right), \end{aligned} \tag{A.20}$$

where the function $\tilde\gamma$ was defined in (50). Now we shift the dummy integration variable according to

$$\begin{aligned}& \int \frac{\mathrm{d}^2 q^\perp}{(2\pi)^2} \to \int \frac{\mathrm{d}^2\kappa^\perp}{(2\pi)^2}, \quad \kappa^\perp = \mathbf{k}_\perp - \mathbf{q}^\perp \\ \Longrightarrow\quad & H^{-+}(x,\xi,t,k_\perp) \\ & = +\mathrm{i}N_c \int \frac{\mathrm{d}^2\kappa^\perp}{(2\pi)^2} \tilde\gamma\left(\kappa^\perp + \frac{\Delta^\perp}{2}, \kappa^\perp - \frac{\Delta^\perp}{2}\right) \\ & \quad \times \int \frac{\mathrm{d}p^+\, \mathrm{d}p^-}{(2\pi)^2} \frac{1}{2p^+p^- - p_1^{\perp 2} - M^2 + \mathrm{i}0} \\ & \quad \times \frac{1}{p^+ - p_1^+ + i0} \frac{1}{\frac{(k_\perp - \kappa_\perp)^2 + M^2}{2p^-} - p_2^+ + \mathrm{i}0} \\ & \quad \times \frac{M^2 - \mathbf{p}_{1\perp}(\mathbf{k}_\perp - \kappa_\perp)}{p^-}. \end{aligned} \tag{A.21}$$

First take the integral over the $p^+$:

$$\begin{aligned}& \int \frac{\mathrm{d}p^+}{(2\pi)} \frac{1}{2p^+p^- - p_1^{\perp 2} - M^2 + \mathrm{i}0} \frac{1}{p^+ - p_1^+ + \mathrm{i}0} = \\ & \quad - \frac{\mathrm{i}\theta(-p^-)}{2p_1^+ p^- - (p_1^\perp)^2 - M^2 + \mathrm{i}0}; \end{aligned} \tag{A.22}$$

next we take the integral over $p^-$:

$$\begin{aligned}\Longrightarrow\quad & H^{-+} \\ & = 2N_c \int \frac{\mathrm{d}^2\kappa^\perp}{(2\pi)^2} \tilde\gamma\left(\kappa^\perp + \frac{\Delta^\perp}{2}, \kappa^\perp - \frac{\Delta^\perp}{2}\right) \\ & \quad \times \frac{M^2 - \mathbf{p}_{1\perp}\cdot(\mathbf{k}_\perp - \kappa_\perp)}{(x+\xi)((\mathbf{k}_\perp - \kappa_\perp)^2 + M^2) - (x-\xi)((\mathbf{p}_1^\perp)^2 + M^2)} \\ & \quad \times \ln\left|\frac{x+\xi}{x-\xi} \frac{(\mathbf{k}_\perp - \kappa_\perp)^2 + M^2}{(\mathbf{p}_1^\perp)^2 + M^2}\right| \\ & = 2N_c \int \frac{\mathrm{d}^2\kappa^\perp}{(2\pi)^2} \tilde\gamma(\kappa^\perp + \frac{\Delta^\perp}{2}, \kappa^\perp - \frac{\Delta^\perp}{2}) \\ & \quad \times \frac{M^2 - \left(\mathbf{k} - \frac{\boldsymbol{\Delta}}{2}\right)\cdot(\mathbf{k}_\perp - \kappa_\perp)}{(x+\xi)((\mathbf{k}_\perp - \kappa_\perp)^2 + M^2) - (x-\xi)\left(\left(\mathbf{k} - \frac{\boldsymbol{\Delta}}{2}\right)^2 + M^2\right)} \\ & \quad \times \ln\left|\frac{x+\xi}{x-\xi} \frac{(\mathbf{k}_\perp - \kappa_\perp)^2 + M^2}{\left(\mathbf{k} - \frac{\boldsymbol{\Delta}}{2}\right)^2 + M^2}\right|. \end{aligned} \tag{A.23}$$

In summary, we have

$$\begin{aligned}& H^{+-} = \\ & 2N_c \int \frac{\mathrm{d}^2\kappa^\perp}{(2\pi)^2} \tilde\gamma\left(\kappa^\perp + \frac{\Delta^\perp}{2}, \kappa^\perp - \frac{\Delta^\perp}{2}\right) \\ & \quad \times \frac{M^2 - \left(\mathbf{k} + \frac{\boldsymbol{\Delta}_\perp}{2}\right)\cdot(\mathbf{k} - \kappa_\perp)}{(x-\xi)((\mathbf{k} - \kappa_\perp)^2 + M^2) - (x+\xi)\left(\left(\mathbf{k} + \frac{\boldsymbol{\Delta}_\perp}{2}\right)^2 + M^2\right)} \\ & \quad \times \ln\left|\frac{x-\xi}{x+\xi} \frac{(\mathbf{k} - \kappa_\perp)^2 + M^2}{\left(\mathbf{k} + \frac{\boldsymbol{\Delta}_\perp}{2}\right)^2 + M^2}\right|, \end{aligned} \tag{A.24}$$

$$\begin{aligned}& H^{-+} = \\ & 2N_c \int \frac{\mathrm{d}^2\kappa^\perp}{(2\pi)^2} \tilde\gamma\left(\kappa^\perp + \frac{\Delta^\perp}{2}, \kappa^\perp - \frac{\Delta^\perp}{2}\right) \\ & \quad \times \frac{M^2 - \left(\mathbf{k} - \frac{\boldsymbol{\Delta}}{2}\right)\cdot(\mathbf{k}_\perp - \kappa_\perp)}{(x+\xi)((\mathbf{k}_\perp - \kappa_\perp)^2 + M^2) - (x-\xi)\left(\left(\mathbf{k} - \frac{\boldsymbol{\Delta}}{2}\right)^2 + M^2\right)} \\ & \quad \times \ln\left|\frac{x+\xi}{x-\xi} \frac{(\mathbf{k}_\perp - \kappa_\perp)^2 + M^2}{\left(\mathbf{k} - \frac{\boldsymbol{\Delta}}{2}\right)^2 + M^2}\right|. \end{aligned} \tag{A.25}$$

Notice that the sum

$$H(x,\xi,t,\mathbf{k}_\perp) = H^{+-}(x,\xi,t,\mathbf{k}_\perp) + H^{-+}(x,\xi,t,\mathbf{k}_\perp) \tag{A.26}$$

is antisymmetric with respect to the inversion of the light-cone fraction $x \to -x$, i.e. $H(-x,\xi,t,\mathbf{k}_\perp) = -H(x,\xi,t,\mathbf{k}_\perp)$.

We can see that in the points $x = \pm\xi$ the result (A.26) has logarithmic divergences $\sim \ln|x \mp \xi|$. Physically, in these points one of the quarks has a zero light-cone fraction, and as a consequence (A.26) becomes very sensitive to the details of the short-distance structure of the model. When we evaluated (A.26), we integrated over $p^\pm$ up to infinity. Rigorously speaking, this contradicts the basic assumptions of the model, in particular (38), which is valid only when the moments of the active partons are much smaller than the moment of the whole nucleus. However, since for $p_{1,2}^+ \neq 0$ the integrals were convergent (the dominant contribution comes from the region where the model is valid), we could ignore such an explicit cutoff. Notice that in the evaluation of the physical DVCS amplitude (54) the cutoffs $|p^-| \leq q^-/2$ were provided by the external kinematics. Generalization of (38) to the more realistic color source is a much more complicated task.

## Appendix B: $\langle U^\dagger U\rangle$-correlator in finite nuclei

As we have seen in the previous section, and as we shall see in the next section, physical observables depend on the correlator

$$\begin{aligned}& \langle P'|U^\dagger(x)U(y)|P\rangle \\ & \quad \approx \bar P^+ \int \mathrm{d}^3 X \mathrm{e}^{\mathrm{i}\boldsymbol{\Delta}\mathbf{X}} \operatorname{Tr}(U^\dagger(x-X)U(y-X)). \end{aligned} \tag{B.1}$$

Notice that the weight functional $W$ is expressed in terms of the field $\rho$, i.e. the correlator is an essentially non-linear object. For a finite nucleus, evaluation of this object

slightly differs from the original derivation given in [21, 22]. However, since the weight functional $W[\rho]$ is Gaussian, the total result can be expressed in terms of the elementary correlator[8] $\langle P'|\rho\rho|P\rangle$.

The final result of our evaluation is

$$\begin{aligned} S(x,y) &= \langle P'|U^\dagger(x_\perp)U(y_\perp)|P\rangle \\ &= \mathrm{e}^{\mathrm{i}\boldsymbol{\Delta}\frac{\mathbf{x}_\perp+\mathbf{y}_\perp}{2}}\int \mathrm{d}^2X \mathrm{e}^{\mathrm{i}\boldsymbol{\Delta}_\perp\mathbf{X}}\exp\Big[-g^2N_c \\ &\quad\times\left(\frac{\tilde f\big(\mathbf{0},\frac{\mathbf{x}_\perp-\mathbf{y}_\perp}{2}-\mathbf{X}\big)+\tilde f\big(\mathbf{0},-\frac{\mathbf{x}_\perp-\mathbf{y}_\perp}{2}-\mathbf{X}\big)}{2}\right. \\ &\quad\left.-\tilde f(\mathbf{x}_\perp-\mathbf{y}_\perp,-\mathbf{X})\Big)\Big]\,, \end{aligned} \tag{B.2}$$

where $\tilde f(\mathbf{r}_1,\mathbf{r}_2)=\int\frac{\mathrm{d}^2\tilde\Delta}{(2\pi)^2}\mathrm{e}^{-\mathrm{i}\tilde\Delta\mathbf{r_2}}\int_{-\infty}^{+\infty}\mathrm{d}z^-\tilde\gamma_A(z^-,\mathbf{r}_1;\tilde\Delta)$.

Indeed, using the definition

$$U(x)=P\exp\left(\mathrm{i}g\int_{-\infty}^{+\infty}\mathrm{d}z^-\alpha^a(z^-,\mathbf{x}_\perp)T_a\right), \tag{B.3}$$

we may notice that

- only even powers of $\alpha$ give a non-zero contribution to (B.2);
- the first term (zero order in $\alpha$) is proportional to $\delta(\Delta)$ and vanishes in the off-forward limit.

The contribution of the second-order term gives

$$\begin{aligned} &-g^2N_c\mathrm{e}^{\mathrm{i}\boldsymbol{\Delta}_\perp\frac{\mathbf{x}_\perp+\mathbf{y}_\perp}{2}}\left(\cos\left(\boldsymbol{\Delta}_\perp\frac{\mathbf{x}_\perp-\mathbf{y}_\perp}{2}\right)\int\mathrm{d}z^-\tilde\gamma_A(z^-,\mathbf{0}_\perp)\right. \\ &\left.-\int\mathrm{d}z^-\tilde\gamma_A(z^-,\mathbf{x}_\perp-\mathbf{y}_\perp;\Delta)\right). \end{aligned} \tag{B.4}$$

It is very convenient to introduce the temporary notation $\int\mathrm{d}z^-\tilde\gamma_A(z^-,\mathbf{r}_\perp;\Delta)=f(\mathbf{r}_\perp;\Delta)$. In this notation (B.4) reduces to

$$-g^2N_c\mathrm{e}^{\mathrm{i}\boldsymbol{\Delta}_\perp\frac{\mathbf{x}_\perp+\mathbf{y}_\perp}{2}}\left(\cos\left(\frac{\boldsymbol{\Delta}_\perp\mathbf{r}_\perp}{2}\right)f(\mathbf{0}_\perp;\Delta)-f(\mathbf{r}_\perp;\Delta)\right), \tag{B.5}$$

where we used the notation $\mathbf{r}=\mathbf{x}_\perp-\mathbf{y}_\perp$.

Evaluation of the higher-order contributions is a bit more tricky. First we have to notice that the Gaussian form of $W[\rho]$ enables us to introduce a sort of Wick theorem for the evaluation of the multileg correlators. After that, we have to make a Fourier transformation of each correlator, take the integral over $\mathrm{d}^2X_\perp$ and make the Fourier transformation back to coordinate space. Performing such a procedure step-by-step, the contribution of the $2n$th order term after some manipulations may be reduced to

$$\begin{aligned} &\sum_{m=0}^{2n}\sum_{k=0}^{\min(m,2n-m)}\frac{(-1)^{n-m}g^{2n}N_c^n}{k!(m-k)!(2n-m-k)!} \\ &\quad\times\int\frac{\mathrm{d}^2\Delta_1^\perp}{(2\pi)^2}\cdots\int\frac{\mathrm{d}^2\Delta_n^\perp}{(2\pi)^2}\delta\Big(\boldsymbol{\Delta}_\perp-\sum_{i=0}^n\boldsymbol{\Delta}_i^\perp\Big) \\ &\quad\times\left(\prod_{i=1}^{\left[\frac{m-k}{2}\right]}f(\mathbf{0},\boldsymbol{\Delta}_i^\perp)\mathrm{e}^{\mathrm{i}\mathbf{x}\boldsymbol{\Delta}_i^\perp}\right) \\ &\quad\times\left(\prod_{i=\left[\frac{m+k}{2}\right]+1}^{n}f(\mathbf{0},\boldsymbol{\Delta}_i^\perp)\mathrm{e}^{\mathrm{i}\mathbf{y}\boldsymbol{\Delta}_i^\perp}\right) \\ &\quad\times\left(\prod_{i=\left[\frac{m-k}{2}\right]+1}^{\left[\frac{m+k}{2}\right]}f(r_\perp,\boldsymbol{\Delta}_i^\perp)\right) \\ &=\mathrm{e}^{\mathrm{i}\boldsymbol{\Delta}\frac{\mathbf{x}_\perp+\mathbf{y}_\perp}{2}}\sum_{m=0}^{2n}\sum_{k=0}^{\min(m,2n-m)}\frac{(-1)^{n-m}g^{2n}N_c^n}{k!(m-k)!(2n-m-k)!} \\ &\quad\times\int\frac{\mathrm{d}^2\Delta_1^\perp}{(2\pi)^2}\cdots\int\frac{\mathrm{d}^2\Delta_n^\perp}{(2\pi)^2}\delta\Big(\boldsymbol{\Delta}_\perp-\sum_{i=0}^n\boldsymbol{\Delta}_i^\perp\Big) \\ &\quad\times\left(\prod_{i=1}^{\left[\frac{m-k}{2}\right]}f(\mathbf{0},\boldsymbol{\Delta}_i^\perp)\mathrm{e}^{\mathrm{i}\mathbf{r}\boldsymbol{\Delta}_i^\perp/2}\right) \\ &\quad\times\left(\prod_{i=\left[\frac{m+k}{2}\right]+1}^{n}f(\mathbf{0},\boldsymbol{\Delta}_i^\perp)\mathrm{e}^{-\mathrm{i}\mathbf{r}\boldsymbol{\Delta}_i^\perp/2}\right) \\ &\quad\times\left(\prod_{i=\left[\frac{m-k}{2}\right]+1}^{\left[\frac{m+k}{2}\right]}f(r_\perp,\boldsymbol{\Delta}_i^\perp)\right). \end{aligned} \tag{B.6}$$

Now we place back

$$\delta\Big(\boldsymbol{\Delta}_\perp-\sum_{i=0}^n\boldsymbol{\Delta}_i^\perp\Big)=\int\mathrm{d}^2X\mathrm{e}^{\mathrm{i}\boldsymbol{\Delta}_\perp\mathbf{X}_\perp}\prod_{i=1}^n\mathrm{e}^{-\mathrm{i}\boldsymbol{\Delta}_i^\perp\mathbf{X}_\perp}$$

and reduce (B.6) to

$$\begin{aligned} &\mathrm{e}^{\mathrm{i}\boldsymbol{\Delta}\frac{\mathbf{x}_\perp+\mathbf{y}_\perp}{2}}\int\mathrm{d}^2X\mathrm{e}^{\mathrm{i}\boldsymbol{\Delta}_\perp\mathbf{X}_\perp} \\ &\quad\times\sum_{m=0}^{2n}\sum_{k=0}^{\min(m,2n-m)}\frac{(-1)^{n-m}g^{2n}N_c^n}{k!(m-k)!(2n-m-k)!} \\ &\quad\times\left(\prod_{i=1}^{\left[\frac{m-k}{2}\right]}\int\frac{\mathrm{d}^2\Delta_i^\perp}{(2\pi)^2}f(\mathbf{0},\boldsymbol{\Delta}_i^\perp)\mathrm{e}^{\mathrm{i}\mathbf{r}\boldsymbol{\Delta}_i^\perp/2}\right) \end{aligned}$$

[8] To check this, just introduce the external current $J\cdot\rho$ and evaluate $\langle P'|\rho_1\ldots\rho_n|P\rangle$ taking derivatives. Notice that this would be not true if we had "interaction terms" $\sim\rho^3,\rho^4$.

$$\times\left(\prod_{i=\left[\frac{m+k}{2}\right]+1}^{n}\int\frac{\mathrm{d}^2\Delta_i^\perp}{(2\pi)^2}f(\mathbf{0},\boldsymbol{\Delta}_i^\perp)\mathrm{e}^{-\mathrm{i}\mathbf{r}\boldsymbol{\Delta}_i^\perp/2}\right)$$
$$\times\left(\prod_{i=\left[\frac{m-k}{2}\right]+1}^{\left[\frac{m+k}{2}\right]}\int\frac{\mathrm{d}^2\Delta_i^\perp}{(2\pi)^2}f(r_\perp,\boldsymbol{\Delta}_i^\perp)\right) \quad (B.7)$$

$$=\mathrm{e}^{\mathrm{i}\boldsymbol{\Delta}\frac{\mathbf{x}_\perp+\mathbf{y}_\perp}{2}}\int\mathrm{d}^2X\mathrm{e}^{\mathrm{i}\boldsymbol{\Delta}_\perp\mathbf{X}}$$
$$\times\sum_{m=0}^{2n}\sum_{k=0}^{\min(m,2n-m)}\frac{(-1)^{n-m}g^{2n}N_c^n}{k!(m-k)!(2n-m-k)!}$$
$$\times\tilde{f}^{\left[\frac{m-k}{2}\right]}\left(\mathbf{0},\frac{\mathbf{r}}{2}-\mathbf{X}\right)\tilde{f}^{\left[\frac{m+k}{2}\right]}\left(\mathbf{0},-\frac{\mathbf{r}}{2}-\mathbf{X}\right)\tilde{f}^{k}(\mathbf{0},-\mathbf{X}) \quad (B.8)$$

$$=\mathrm{e}^{\mathrm{i}\boldsymbol{\Delta}\frac{\mathbf{x}_\perp+\mathbf{y}_\perp}{2}}\int\mathrm{d}^2X\mathrm{e}^{\mathrm{i}\boldsymbol{\Delta}_\perp\mathbf{X}}\exp\left[-g^2N_c\right.$$
$$\left.\times\left(\frac{\tilde{f}\left(\mathbf{0},\frac{\mathbf{r}}{2}-\mathbf{X}\right)+\tilde{f}\left(\mathbf{0},-\frac{\mathbf{r}}{2}-\mathbf{X}\right)}{2}-\tilde{f}(\mathbf{r},-\mathbf{X})\right)\right], \quad (B.9)$$

in agreement with (B.2).

For the evaluation of the complicated objects like

$$\langle P'|\Phi[\rho]U^\dagger(x_\perp)U(y_\perp)|P\rangle$$

(see e.g. the gluon distributions) we can use a quasiclassical formula:

$$\langle P'|\hat{A}(x,y)\hat{B}(x,y)|P\rangle$$
$$=\frac{\mathrm{e}^{\mathrm{i}\boldsymbol{\Delta}\frac{\mathbf{x}+\mathbf{y}}{2}}}{\bar{P}^+}\int\mathrm{d}^3X\mathrm{e}^{\mathrm{i}\boldsymbol{\Delta}\mathbf{X}}$$
$$\times\left(\int\frac{\mathrm{d}^3\Delta_1}{(2\pi)^3}\mathrm{e}^{-\mathrm{i}\boldsymbol{\Delta}_1\mathbf{X}}\left\langle P+\Delta_1\left|\hat{A}\left(\frac{\mathbf{r}}{2},-\frac{\mathbf{r}}{2}\right)\right|P\right\rangle\right)$$
$$\times\left(\int\frac{\mathrm{d}^3\Delta_2}{(2\pi)^3}\mathrm{e}^{-\mathrm{i}\boldsymbol{\Delta}_2\mathbf{X}}\left\langle P+\Delta_2\left|\hat{B}\left(\frac{\mathbf{r}}{2},-\frac{\mathbf{r}}{2}\right)\right|P\right\rangle\right)$$
$$=\frac{\mathrm{e}^{\mathrm{i}\boldsymbol{\Delta}\frac{\mathbf{x}+\mathbf{y}}{2}}}{\bar{P}^+}\int\frac{\mathrm{d}^3\Delta_1}{(2\pi)^3}\frac{\mathrm{d}^3\Delta_2}{(2\pi)^3}(2\pi)^3\delta^3(\Delta-\Delta_1-\Delta_2)$$
$$\times\left\langle P+\Delta_1\left|\hat{A}\left(\frac{\mathbf{r}}{2},-\frac{\mathbf{r}}{2}\right)\right|P\right\rangle\left\langle P+\Delta_2\left|\hat{B}\left(\frac{\mathbf{r}}{2},-\frac{\mathbf{r}}{2}\right)\right|P\right\rangle$$
$$=\mathrm{e}^{\mathrm{i}\boldsymbol{\Delta}\frac{\mathbf{x}+\mathbf{y}}{2}}\int\mathrm{d}^3X\mathrm{e}^{\mathrm{i}\boldsymbol{\Delta}\mathbf{X}}A^{\mathrm{cl}}\left(\frac{\mathbf{r}}{2}-\mathbf{X},-\frac{\mathbf{r}}{2}-\mathbf{X}\right)$$
$$\times B^{\mathrm{cl}}\left(\frac{\mathbf{r}}{2}-\mathbf{X},-\frac{\mathbf{r}}{2}-\mathbf{X}\right), \quad (B.10)$$

where $\mathbf{r}=\mathbf{x}-\mathbf{y}$.

## References


1. D. Mueller, D. Robaschik, B. Geyer, F.M. Dittes, J. Horejsi, Fortschr. Phys. **42**, 101 (1994) [arXiv:hep-ph/9812448]
2. X.D. Ji, Phys. Rev. D **55**, 7114 (1997)
3. X.D. Ji, J. Phys. G **24**, 1181 (1998) [arXiv:hep-ph/9807358]
4. A.V. Radyushkin, Phys. Lett. B **380**, 417 (1996) [arXiv:hep-ph/9604317]
5. A.V. Radyushkin, Phys. Rev. D **56**, 5524 (1997)
6. A.V. Radyushkin, arXiv:hep-ph/0101225
7. X.D. Ji, J. Osborne, Phys. Rev. D **58**, 094018 (1998) [arXiv:hep-ph/9801260]
8. J.C. Collins, A. Freund, Phys. Rev. D **59**, 074009 (1999)
9. J.C. Collins, L. Frankfurt, M. Strikman, Phys. Rev. D **56**, 2982 (1997)
10. S.J. Brodsky, L. Frankfurt, J.F. Gunion, A.H. Mueller, M. Strikman, Phys. Rev. D **50**, 3134 (1994)
11. K. Goeke, M.V. Polyakov, M. Vanderhaeghen, Prog. Part. Nucl. Phys. **47**, 401 (2001) [arXiv:hep-ph/0106012]
12. M. Diehl, T. Feldmann, R. Jakob, P. Kroll, Nucl. Phys. B **596**, 33 (2001) [arXiv:hep-ph/0009255]
13. M. Diehl, T. Feldmann, R. Jakob, P. Kroll, Nucl. Phys. B **605**, 647 (2001) [Erratum]
14. A.V. Belitsky, D. Mueller, A. Kirchner, Nucl. Phys. B **629**, 323 (2002) [arXiv:hep-ph/0112108]
15. M. Diehl, Phys. Rep. **388**, 41 (2003) [arXiv:hep-ph/0307382]
16. A.V. Belitsky, A.V. Radyushkin, Phys. Rep. **418**, 1 (2005) [arXiv:hep-ph/0504030]
17. Jefferson Lab Hall A Collaboration, C. Munoz Camacho et al., Phys. Rev. Lett. **97**, 262002 (2006) [arXiv:nucl-ex/0607029]
18. F. Ellinghaus, arXiv:0710.5768 [hep-ex]
19. K. Goeke, V. Guzey, M. Siddikov, Eur. Phys. J. A **36**, 49 (2008) [arXiv:0802.0669 [hep-ph]]
20. L.V. Gribov, E.M. Levin, M.G. Ryskin, Phys. Rep. **100**, 1 (1983)
21. L.D. McLerran, R. Venugopalan, Phys. Rev. D **49**, 2233 (1994) [arXiv:hep-ph/9309289]
22. L.D. McLerran, R. Venugopalan, Phys. Rev. D **49**, 3352 (1994) [arXiv:hep-ph/9311205]
23. K.J. Golec-Biernat, Acta Phys. Pol. B **35**, 3103 (2004)
24. E. Iancu, K. Itakura, L. McLerran, Nucl. Phys. A **724**, 181 (2003) [arXiv:hep-ph/0212123]
25. E. Iancu, R. Venugopalan, arXiv:hep-ph/0303204
26. G.A. Miller, J.R. Smith, Phys. Rev. C **65**, 015211 (2002) [arXiv:nucl-th/0107026]
27. G.A. Miller, J.R. Smith, Phys. Rev. C **66**, 049903 (2002) [Erratum]
28. M. Froissart, Phys. Rev. **123**, 1053 (1961)
29. V.N. Gribov, Sov. Phys. JETP **30**, 709 (1970)
30. V.N. Gribov, Zh. Eksp. Teor. Fiz. **57**, 1306 (1969)
31. L. Frankfurt, V. Guzey, M. McDermott, M. Strikman, Phys. Rev. Lett. **87**, 192301 (2001) [arXiv:hep-ph/0104154]
32. J. Bartels, B.I. Ermolaev, M.G. Ryskin, Z. Phys. C **70**, 273 (1996) [arXiv:hep-ph/9507271]
33. J. Bartels, B.I. Ermolaev, M.G. Ryskin, Z. Phys. C **72**, 627 (1996) [arXiv:hep-ph/9603204]
34. A. De Rujula, S.L. Glashow, H.D. Politzer, S.B. Treiman, F. Wilczek, A. Zee, Phys. Rev. D **10**, 1649 (1974)
35. E.A. Kuraev, L.N. Lipatov, V.S. Fadin, Sov. Phys. JETP **44**, 443 (1976)
36. E.A. Kuraev, L.N. Lipatov, V.S. Fadin, Zh. Eksp. Teor. Fiz. **71**, 840 (1976)
37. I.I. Balitsky, L.N. Lipatov, Sov. J. Nucl. Phys. **28**, 822 (1978)
38. I.I. Balitsky, L.N. Lipatov, Yad. Fiz. **28**, 1597 (1978)
39. E.A. Kuraev, L.N. Lipatov, V.S. Fadin, Sov. Phys. JETP **45**, 199 (1977)

40. E.A. Kuraev, L.N. Lipatov, V.S. Fadin, Zh. Eksp. Teor. Fiz. **72**, 377 (1977)
41. K.J. Golec-Biernat, M. Wusthoff, Phys. Rev. D **59**, 014 017 (1999) [arXiv:hep-ph/9807513]
42. C.S. Lam, G. Mahlon, Phys. Rev. D **61**, 014 005 (2000) [arXiv:hep-ph/9907281]
43. Y.V. Kovchegov, Phys. Rev. D **54**, 5463 (1996) [arXiv: hep-ph/9605446]
44. S. Jeon, R. Venugopalan, Phys. Rev. D **71**, 125 003 (2005) [arXiv:hep-ph/0503219]
45. V.N. Gribov, A.A. Migdal, Sov. J. Nucl. Phys. **8**, 583 (1969)
46. V.N. Gribov, A.A. Migdal, Yad. Fiz. **8**, 1002 (1968)
47. J.B. Bronzan, G.L. Kane, U.P. Sukhatme, Phys. Lett. B **49**, 272 (1974)
48. D.P. Sidhu, U.P. Sukhatme, Phys. Rev. D **11**, 1351 (1975)
49. L.D. Faddeev, V.E. Korepin, Phys. Rep. **42**, 1 (1978)
50. H. Kowalski, D. Teaney, Phys. Rev. D **68**, 114 005 (2003) [arXiv:hep-ph/0304189]
51. P. Pobylitsa, Comments on the color glass condensate, unpublished
52. K. Hencken et al., Phys. Rep. **458**, 1 (2008) [arXiv: 0706.3356 [nucl-ex]]
53. A. Baltz et al., arXiv:hep-ph/0702212